CRYOGENIC DRILLING OF KEVLAR™ COMPOSITE LAMINATES

BY

MUJAHED AHMED

A Thesis Presented to the

DEANSHIP OF GRADUATE STUDIES

KING FAHD UNIVERSITY OF PETROLEUM & MINERALS

DHAHRAN, SAUDI ARABIA

In Partial Fulfillment of the
Requirements for the Degree of

MASTER OF SCIENCE

In

MECHANICAL ENGINEERING

December 2004

KING FAHD UNIVERSITY OF PETROLEUM & MINERALS
DHAHRAN 31261, SAUDI ARABIA

DEANSHIP OF GRADUATE STUDIES

This thesis, written by **MUJAHED AHMED** under the direction of his Thesis Advisor and approved by his Thesis Committee, has been presented to and accepted by the Dean of Graduate Studies, in partial fulfillment of the requirements for the degree of **MASTER OF SCIENCE IN MECHANICAL ENGINEERING.**

Thesis Committee

Dr. AbdelRahman N. Shuaib (Chairman)

Dr. Al-Sulaiman, Faleh A. (Co-Chairman)

Dr. NeÇar Merah (Member)

Dr. Al-Sulaiman, Faleh A
(Department Chairman)

Dr. Rached Ben-Mansour (Member)

Dr. Mohammad Abdul-Aziz Al-Ohali
(Dean of Graduate Studies)

Dr. Abul Fazal M. Arif (Member)

١٤٢٦/٥/٢٧هـ

Date
4-7-2005

عمادة الدراسات العليا
DEANSHIP OF GRADUATE STUDIES

ACKNOWLEDGEMENT

In the name of Allah, Most Gracious, Most Merciful

I thank Allah (subhana hu wa taala) for bestowing me with health, knowledge and patience to complete this work. Thereafter, acknowledgement is due to KFUPM for the support given for this research through its tremendous facilities and for granting me the opportunity to pursue graduate studies with financial support.

I acknowledge, with deep gratitude and unrestrained appreciation my Committee Chairmen, Dr. AbdelRahman N. Shuaib, for his inspiration, encouragement and guidance throughout. Special thanks are due to Co-Chairmen Dr. Faleh Al-Sulaiman for providing me the workpiece material for the experiments. I also thank Dr. Neçar Merah, for his continuous moral support, help, encouragement and guidance during this research work and Dr. Rached Ben-Mansour & Dr. Abul Fazal M. Arif, for their help and valuable advices. Thanks are due to Mr. Inam Muhammad for his solemn help in thermal measurements and Mr. Hashmi, M. Lateef for his continuous support in material science lab. I also acknowledge the efforts of Mr. Kamal Ali, Mr. Saber Ali and rest of the ME-workshop staff during my experiments.

Special thanks are due to my colleagues at the university, Ameen, Kaleem, Junaid, Zaheer, Shafi, Abbas, Riyaz, Moied Bhai, Sohail, Noman, Sanaullah and Faheem who always helped me and provided a wonderful company. Finally, thanks are due to my parents and to my sisters for their emotional and moral support throughout my academic career and also for their love, patience, encouragement and prayers.

ABSTRACT (ENGLISH)

FULL NAME OF STUDENT:	MUJAHED AHMED
TITLE OF STUDY:	CRYOGENIC DRILLING OF KEVLAR™ COMPOSITE LAMINATES
MAJOR FIELD:	MECHANICAL ENGINEERING
DATE OF DEGREE:	DECEMBER, 2004

Cryogenic machining is gaining increasing acceptance in metal industries and is replacing the conventional machining processes to overcome the shortcomings of the conventional coolants. Materials like aramid fibre reinforced composite are difficult to machine because of the unique combination of physical properties of fibre and the matrix. The present study evaluates the machinability of Kevlar™-49 composite laminates at low temperatures using TiN coated HSS drill.

The effects of workpiece temperature and cutting conditions on machinability of laminates were assessed using drilling thrust force, cutting torque, specific energy and hole quality. Both workpiece temperature and machining conditions were found to influence each of maximum thrust force, maximum torque and specific cutting energy at different levels. Both drilling thrust and torque showed increasing trend with decrease in the workpiece temperature under all machining conditions. Drilled hole patterns of the laminates obtained using optical technique showed less fibre protrusion and delamination at low temperatures compared to ambient. An improvement of about 400% was observed when the workpiece temperature was reduced from 20^0C to -120^0C.

ABSTRACT (ARABIC)

ملخص الرسالة

الاســـــــــم: مجـــــــاهـد أحـــــمـــــــــــد

عنوان الرسالة: الـــحفـــــر الـــبـــــــارد لKEVLAR^{TM}

التخصـــــص: الهـــــنـــــــدسـة المـــــيـــــكـــانـــيـــكـــيـــة

تاريخ التخـرج: ديسمبر 2004

لقد ازدادت أهمية المكائن اللتي تعمل بالتبريد في الصناعات المعدنية وبدأت تحل محل المكائن التقليدية للتغلب على عيوب المبردات التقليدية. إن مواد مثل فايبر الأراميد المركب والمدعم من الصعوبة بمكان أن تصنع بسبب الخواص الفريدة الممثلة في الصفات الفيزيائية لكل من الفايبر والمكونات الداخلة في تركيبه. إن الدراسة الحالية تقيم تصنيع Kevlar^{TM}-49 المركب من صفائح عند درجة حرارة منخفضة باستخدام TiN coated HSS drill.

تم تقييم تأثير كل من درجة الحرارة و ظروف القطع عملية تصنيع الصفائح عن طريق قوة الحفر الدفعي ، عزم القطع ، الطاقة الفعالة و جودة الثقب. ولقد وجد إن كلا من حرارة القطعة المشغولة و ظروف التصنيع تؤثر على كل من القوة الدفعية القصوى ، العزم الأقصى ، طاقة القطع الفعالة بمستويات متفاوتة. تم اختبار الفرضية لدراسة تأثير خفض حرارة القطعة المشغولة على قوة التصنيع و جودة الثقب. ولقد أظهر كلا من الحفر الدفعي و العزم زيادة طردية مع خفض حرارة القطعة المشغولة بسبب هشاشة الصفائح عند درجات الحرارة المنخفضة. ولقد أظهرت الثقوب المحفورة للصفائح واللتي تم الحصول عليها بالتقنيات البصرية وجود نتوءات وتشققات أقل للصفائح عند درجات حرارة منخفضة مقارنة مع درجة المحيط العادية. وتم ملاحظة تحسن مقداره 400% عندما تم خفض درجة الحلرارة المشغولة إلى 120 درجة مئوية تحت الصفر مقارنة مع حرارة الغرفة.

TABLE OF CONTENTS

LIST OF FIGURES

LIST OF TABLES

CHAPTER 1

INTRODUCTION

1.1 General Background

All machining processes generate and transfer heat, primarily through friction and plastic deformation. This heat is of concern both to the manufacturing engineer, who is concerned about the effects of heat on the process capability, and to the environmental engineer, who must look at all environmental effects from the process. High cutting temperature in machining not only impairs the dimensional and form accuracy, but also affects the surface integrity of the product by inducing residual stresses and surface and subsurface cracks [44].

Historically, cutting fluids have been used extensively for the last 200 years. Cutting fluids are widely utilized to improve the process of machining operations such as turning, drilling, boring, grinding, and milling. The most common metalworking fluids used today are either oil-based fluids including straight oils and soluble oils or chemical fluids including synthetics and semi-synthetics. The primary function of cutting fluid is temperature control through cooling and lubrication. Cooling and lubrication are critical

in decreasing tool wear, extending tool life and achieving the desired size, finish and shape of the workpiece. A secondary function of cutting fluid is to flush away chips and metal fines from the tool/workpiece interface to prevent a finished surface from becoming marred and also to reduce the occurrence of built-up edge (BUE). Monitoring and maintenance of cutting fluid is required due to contamination and degradation. Eventually, fluids require disposal once their efficiency is lost. Waste management and disposal become a major problem concerning environmental liability. The primary concern is the significant negative effects to worker's health associated with use of the cutting fluids [52].

In order to minimize the negative effects of the conventional cutting fluids new alternative is now gaining increasing acceptance in the metal industries i.e. the use of cryogenics as a coolant and lubricant. Cryogenics machining makes use of special mechanical properties of materials in a cryogenic or a 'super cold' state of machining [18]. The research work in developing this technology started few decades back when attempts were made to replace the conventional cooling methods with cryogenics. Today scientists and metallurgists are using cryogenics in a number of fields including industrial applications, life sciences, physical research, breeding etc. [53]. While the cryogenics industry is well established, the use of cryogenics in the metal-cutting industry is relatively new. It has been realized that many materials can be machined more easily if they are cooled below room temperature-for example, by using liquid nitrogen as a coolant. This appears to be more attractive for composite materials. Composite materials provide distinctive advantages in the manufacture of advanced products because they have

attractive features, such as high ratios of strength-to-weight and stiffness-to-weight. Unlike most of the engineering materials, polymeric composites are characterized by the marked anisotropy, structural inhomogenity and lack of plastic deformation behavior. They can, however, be easily damaged when machined unless the machining process is performed properly. The typical damage undergone by laminated composites is delamination caused by machining processes. There are two important types of polymer matrix composites, short-fiber and continuous-fiber composites. The choice of polymer matrix for such composites can be either a thermoset or a thermoplastic. Continuous-fiber composites that offer the best mechanical properties compared to other fiber-reinforced composites are primarily reinforced with high performance fiber composite matrix resins such as carbon or aramid fiber (Kevlar^{TM}) and are often utilized in special applications like aircraft components in which the property benefits of the fibers are fully exploited [54]. Aramid fibers are very important reinforcement for advanced composites.

Kevlar^{TM} aramid fiber was commercialized by Du Pont Company in 1972 as an industrial fibre product. 'Kevlar^{TM}" is registered trademark of Du Pont Co. The term 'aramid' is common term for 'a manufactured fiber in which the fiber-forming material is a long chain synthetic polyamide in which at least 85% of the amide linkages are attached directly two aromatic rings' the discovery of Kevlar^{TM} aramid fiber began in 1965 when S. L. Kwolek, a Du Pont research scientist, synthesized a series of para-oriented aromatic polyamides [55].

General features of Kevlar include: high tensile strength at low weight, low elongation to breakage, high modulus (structural rigidity), low electrical conductivity,

high chemical resistance, low thermal shrinkage, high toughness (work-to-break), self-extinguishing. Composites reinforced with Kevlar™ have been developed rapidly for many applications in advanced materials. These applications make use of the high tensile strength and modulus, light weight, thermal and dimensional stability, and other unique properties of Kevlar™ aramid fiber. High modulus Kevlar™ 49 and Kevlar™ 149 aramid fibers are suitable reinforcement fibers for composites. The major advantage of composites reinforced with Kevlar™ versus those with glass and carbon fibers are the light weight, high tensile strength and modulus, outstanding toughness and high impact resistance. Kevlar™ reinforced composites are employed on a wide range of product applications. They include aircraft and aerospace, pressure vessels, automotive parts, protruded articles, ships, and boats, friction products, sporting goods, and aramid/aluminum laminates.

1.2 Drilling of Fiber Reinforced Plastics

Fibre Reinforced Plastics (FRP) composites occupy an important place as high performance engineering materials. For certain types of composites where the fabrication method precludes the ability to mold in the holes, drilling is the only acceptable method. But drilling holes in laminated composites is a challenge. Their highly abrasive nature quickly dulls high speed steel and carbide tools, and their low interlaminar strength often results in splintering and delamination of the hole [23]. Although in most of the fabrication processes used for composites, machining is avoided, sometimes machining of

FRP is essential. Out of various machining processes used for FRP, drilling is the most common machining operation [21]. The technical literature of drilling of fiber-reinforced plastics reports that the quality of the machined parts is strongly dependent on drilling parameter. Drilling induced delamination occurs both at the entrance and the exit planes of the workpiece. The drill geometry is considered as the most important factor that affects drill performance [30]. Several non-traditional machining processes, i.e. laser-beam drilling, water-jet drilling (with or without abrasives), ultrasonic drilling, electrical discharge machining (EDM), have been reported as alternatives. Nevertheless, conventional drilling continues to be widely used for practical & economical purposes. Various drilling tools are available, but the twist drill is by far the most common. The rotation and feeding of the drill bit results in relative motion between the cutting edges and the workpiece to produce chips. The efficiency of the cutting action varies, being the most efficient at the outer diameter of the drill where the rake angle is positive and the least efficient at the center where the rake angle becomes negative. In fact, the relative velocity at the drill point is zero, without cutting action. Instead, the chisel edge of the drill point pushes aside the material at the center as it penetrates into the hole by extrusion. Several specialized drills were developed to reduce the delamination.

The drilling of holes in FRP composites presents problems different from those encountered in drilling metals and alloys. Problems encountered in drilling of FRP composites include [3]:

- FRPs are machinable only in a limited range of temperature. Even though the fibers will withstand higher temperatures, the curing temperature of the resin should not be exceeded to avoid material disintegration.
- The low thermal conductivity favors heat build-up in the cutting zone during machining operations, since there is only little dissipation into the material. The greatest part of the heat has to be carried away through the tool and thus affect tool wear and life.
- The difference in coefficients of thermal expansion between matrix (highly positive) and fiber (slightly negative for carbon and aramid) is favorable for the formation of residual stress and makes it difficult to attain high dimensional accuracy. Drilled holes, for example, often show a smaller diameter than the drill used.
- Reinforced fibers and fillings may cause a highly abrasive tool wear, which restricts the selection of utilizable cutting material.
- The change of physical properties by absorption of fluids is only insufficiently known, this has to be considered when deciding to use a coolant.
- Crack formation and Surface roughness.
- Damage to surface layers (delamination).
- Deviation of hole diameter from nominal diameter (hole shrinkage) and roundness error.

Drilling FRP using conventional fluids is not a recommended practice because of their high moisture absorbing abilities. Usually FRP are drilled without any coolant either by sacrificing the tool or restricting the machining parameters to less than optimum condition

in order to achieve the desired output. When cryogenic machining was introduced to machine tough metals and alloys, composite materials were not far behind in the race because of the preceding reasons. Scientists and researchers started using cryogenic coolants such as liquid Nitrogen (LN_2) to machine composite materials. The challenging task that faces the researchers for cryogenic machining is to design an effective cooling system and to find an optimal balance between the improvement in machinability and negative effect LN_2 can put on the tool. The various cooling techniques implemented include pre-chilling the workpiece and tool material, flooding the work-tool contact area with coolant (like conventional cooling), cooling the selected regions of work-tool interface, cooling only the tool while machining, cooling only the workpiece while machining etc. [20]. Proper design of cooling system is important as it affects the machinability of the workpiece. The most efficient cooling system will be the one that can apply the coolant near to the work-tool interface where the heat generation is large. This can be done easily for machining processes in which the tool contact region is fully exposed like turning, milling, grinding etc. As far as drilling is concerned it is quite difficult to reach exactly the location where the cutting edge of the drill is in contact with that of work material. So for drilling, cryogenic cooling is accomplished either by cooling the tool or work before or during machining. This usually requires a relatively complex cooling system.

1.3 Research Objectives

The overall goal or the objective of this study is to evaluate the effect of cryogenic cooling on machinability of Kevlar 49 fiber reinforced composites. The efforts are directed towards understanding the effects of cryogenic cooling and the machining parameters such as feed and speed on the cutting behavior using commercially available Titanium Nitrate (TiN) coated High Speed Steel (HSS) drills. Drilling experiments are conducted on aramid composites laminates under different workpiece temperatures. The performance parameters for evaluation of machinability include cutting forces, specific energy and the hole quality in terms of delamination and fibre breakage of the machined surface.

To meet the above objectives, an experimental program was devised. The results of this experimental study are presented in this thesis. The thesis organization is as follows: Chapter 2 provides a detailed literature review and Chapter 3 covers the design of the experimental setup and methodology of the experiments performed to generate the data required for evaluating the machinability of Kevlar Aramid fiber. The detailed results and discussions of thrust force, cutting torque and specific cutting energy are explained in Chapter 4. Chapter 5 discusses the effect of cryogenic cooling on drilled hole quality while Chapter 6 contains conclusions and recommendations

CHAPTER 2

LITERATURE REVIEW

Uehara and Kumagai, [1] made an initial effort towards studying fundamentally the effects of cryo-machining. They performed series of experiments on different types of workpiece and machined them using liquid nitrogen (LN_2) coolant. Decreases in size of build up edges were observed resulting in improved surface roughness. Experiments showed that the cutting performance during cryo-machining exhibits complicated tendencies that depend upon the combinations of cutting and cooling conditions and also the type of workpiece and tool used.

Jainbajranglal and Chatopadhyay [2] discussed the suitability and applicability of liquid nitrogen (LN_2) as coolant during machining, they observed the beneficial effects of cryogenic machining in reducing the cutting forces and power requirements, and apart from this they reported a marked improvement in tool life, dimensional accuracy and tool failure reduction. The main objective of their study was to investigate and compare cryo-turning and cryo-grinding with their conventional counter parts using soluble oil as coolant with respect to grinding forces, grinding temperature and surface quality of the machined part. A specially built nozzle was used to spray the jet of pressurized LN_2 on the

tool workpiece interface. A low carbon steel material was turned using cryogenic coolant,and improvement in surface finish with little traces of micro tearing and cracks were observed compared to the conventional turning at high speeds and feeds. But the degree of tool wear reduction varied with cutting conditions. Reduction in cutting forces was observed due to partial transformation of shear deformation of the chip into brittle fracture and reduction in stagnation tendency of chip material and formation of 'Built up Edge' (BUE). During cryogenic grinding substantial decrease in both temperature and force were observed compare to conventional grinding along with smoother machined surfaces free from micro cracks. They concluded that machining carbon steel using LN_2 decreases the cutting forces and tool wear and improves surface integrity.

Hocheng and Dharan [3] studied the phenomenon of delamination damage produced during the drilling of CFRP. They proposed a model that related the delamination of the laminate to drilling parameters and composite properties. The analysis used a fracture mechanics approach in which the opening mode delamination fracture toughness, a material parameter, was used with a plate model of the laminate. The analysis predicted an optimal thrust force (defined as the minimal thrust force above which delamination is initiated) as a function of drilled hole depth. An advantage of their model was that it could predict varying degrees of delamination for other materials, such as glass fiber-epoxy and for hybrid composites.

The attempts made in the past to machine Kevlar Aramid fiber reinforced plastics (KFRP) with the conventional cutting tools were difficult and didn’t received much success. A novel technique has been designed by Bhattacharyya, Allen, and Mander [4] to

machine the KFRP under cryogenic cooling conditions. They analyzed the machinability, cutting speed and tool geometry during turning of KFRP composite material with surface finish of the machined workpiece as a criterion in determining the tool life. They established a suitable temperature range for cryo-machining.

The cryogenic condition can be achieve either by soaking the workpiece in LN_2 for a predetermined period and then machining upon removal or by directly applying the coolant onto the workpiece while machining, mostly the latter option provides far superior results with low additional costs and a provision for long continuous machining. Microscopic investigation revealed that under cryogenic machining conditions the fiber matrix combination behaves in a more rigid fashion thus producing the less bending and pullout of Kevlar fibers. The tool used with continually pouring LN_2 at a flow rate of 0.4-0.5 l/mm showed satisfactory performance, the tool material exhibits mild strap wear on primary and secondary cutting edges with slight rounding of former, whereas the flank wear growth was observe to vary inversely with the cutting speed Reduction in cutting forces were observed due to the fact that resin and matrix have different thermal expansion coefficient in both the directions that produces compressive stress (clamping force) in the fibers reducing their deflection and shear fracture failure thereby producing cleaner cuts. Surface finish is strongly influenced by the temperature of the workpiece and best finish was achieved when LN_2 was poured continuously during machining Another peculiarity of machining the KFRP is the remnant of uncut fibers left on un-machined side of the workpiece and the uncut fiber length increases with temperature, this fuzziness is difficult to quantify but a low cutting speed will give a better surface finish.

Hong [5] discusses the advantages of cryo-machining over conventional machining method and studied the effects of different machining aspects like tool wear, thermal-conductivity, and machinability, economical and environmental impact. He also discussed the mechanisms with which the formation of BUE during machining can be minimized. Composite materials were machined using cryo coolant as composites are generally abrasive with low thermal conductivity and causes severe tool wear, tool and workpiece burns at elevated temperatures and non availability of suitable cutting fluids for machining due to constraints and difficulty in after work cleaning.

Evans [6] discusses the turning of ferrous materials with single point diamond tool focusing mainly on tool wear mechanisms like adhesion and formation of build up edges, abrasion, micro chipping, fracture and fatigue and tribo thermal and tribo chemical wears. Specially designed cooling system has been developed that cools the tool shank clamped onto the special purpose tool holder designed to minimize the heat flux from the tool with the rear of the tool shank immersed in LN_2 reservoir. A special chuck was also designed through which LN_2 was supplied using stationary supply tube that hits the front face of the reservoir thereby throwing out the coolant centrifugally without stopping the spindle while the chuck is in operation. The results showed decreased tool wear and better surface finish.

DiIlio et al [7] performed drilling experiments of Aramid fiber composite. Relationships have been evidenced between the trends of the thrust force and the torque with regard to the tool bit geometry and the composite structure for different feed rates and for different composite constructions. He found a continuous decrease of the mean

value of the thrust force, which has been attributed to the heat build-up at the cutting front. The torque was found to be strongly influenced by friction at the lands of the twist drill. The trends of the thrust force as a function of hole depth were reported. It showed that after a transient stage, during which the thrust force regularly increases up to a maximum corresponding to the complete engagement of the tool bit, a larger period could be noticed which was relative to the cutting of bulk material. In this second stage the force had a very irregular trend around a mean value which tended to decrease as the machining proceeded, until the tool exit. At high feed rates the values of the forces were higher with respect to the one obtained at lower feed rates. The continuous decrease of the thrust force during drilling can be attributed to the reduction of the material strength as a consequence of the temperature increased at the cutting front.

Zhao and Hong [8, 9] presented their arguments on response of different materials to the temperature during machining and discussed different cooling strategies for improved machinability of materials during machining. Different steels along with aluminum and titanium alloys were machined to investigate the Cryo-machining process. The experiments showed that machining pre-chilled low carbon steels resulted in increased hardness and strength, decreased toughness, better chip formation with reduction in cutting forces, and increased in chip breakability due to low temp brittleness, while it has a reverse effect when the high carbon and bearing steels were machined pre-chilled, therefore the coolant has to be applied to the cutting zone while machining in order to achieve better results. For cast aluminum alloy the hardness and resistance to abrasive wear can be enhanced by cooling the cutting tool with Cryogenic coolants. For

machining titanium and its alloys it is difficult to adopt a cooling strategy based on the its properties, but effective strategy will be to cool the workpiece and the tool simultaneously, thus lowering the high cutting temperatures developed during the machining and also enhancement in the chemical stability of the workpiece and cutting tool. Therefore cryogenic machining is expected to give greater potential in high productivity machining of titanium and its alloys. They also discussed about the cutting tool material properties during machining whether they will be able to maintain their strength and toughness and withstand the low temperature shock during cryogenic cooling.

These authors [9] also explained the cryogenic cooling strategies and optimum machining conditions. They performed micro structural observations along with impact testing, transverse rupture strength and indentation test that shows that, the carbide tool materials posses good Cryo properties but certain grades exhibits the reversed tendencies to cryo-machining whereas the HSS tool material showed increased hardness and decreased impact strength during Cryo-machining.

Hocheng and Pwu [10, 12, 13] found that during machining the cutting chips produced by thermoplastic material shows a large amount of deformation in chip formation, while thermoset tend to be fractured. Such a difference in cutting mechanism also explained the different surface quality achieved. A Carbon/ABS composite was found to be superior than carbon/epoxy ones for both quality of hole edges and walls. An examination of the specific cutting energy suggested that the effect of chip size existed for both materials with various degree of strength.

Bhattacharyya et al. [11] described a novel technique of machining KFRP composites under cryogenic cooling. They investigated the effects of various machining parameters such as workpiece temperature, cutting speed, and tool geometry on machinability of KFRP composites. The criterion selected for determining the tool performance was surface finish and microscopic investigation of the cutting zone of machining mechanics under ambient and cryogenic temperature is also discussed.

The cryogenic conditions were achieved either by pre cooling the workpiece for pre determined time or continual pouring of the LN_2 onto the workpiece while machining, the latter technique has been found to be more effective. Three different temperature ranges were selected for cooling during machining, range 1; -195^0C to -185^0C, range 2; -135^0C to -103^0C and range 3; -75^0C to -60^0C. But the experiments were carried out mostly in range 1 by continual pouring of coolant onto the workpiece at a flow rate of 0.4-0.5 l/min.

During machining three main machinability criterion were recorded which includes flank wear, tool forces and surface finish. Micromachining has been performed considering ambient and low temperature situations, the latter was achieved by applying LN_2 with cotton swabs onto KFRP wafer kept under microscope with stationary cutting tool clamped beneath it, the process was recorded with the aid of video recording.

The results obtained showed that due to continual rubbing of loosened fibers, chip notching, edge rounding and higher temperatures take place, which increases the cutting force and causes severe deterioration of surface finish. When LN_2 was poured continually during machining a mild strap wear on the primary and secondary cutting edges with

slight primary edge rounding was observed. Cryogenic coolant didn't show any remarkable effects on the tool forces at initial stage but after a certain period of machining time the differences were noticed which are due to the differences in the thermal expansion coefficients of resins and matrix which also causes a compressive induced stress in the fibers producing a clamping force which combined with epoxy and becomes stiffer thereby reducing fiber deflection causing failure mode change from induced bending rupture to shear fracture producing cleaner cuts. The surface finish of the machined surface using cryogen exhibits low fuzzy texture compare to dry machining with best finish obtained due to continual pouring of LN_2.

Wrong machining of composites leads to delamination, burning, local cracks, fiber pull-out, fiber not being cut, high surface roughness and thereby final rejection by inspection. Bhatnagar et al. [14] used the technique of dimensional analysis to investigate the complex correlation among some of the major parameters responsible for drill performance in FRP drilling. They found that the composite material has a non-homogeneous (anisotropic) structure and its machinability is quite different from that of homogeneous (isotropic) material such as steel or cast iron. As per literature higher cutting speeds were recommended for FRP, but in their research the authors found that the best clean cut hole was obtained at 500 rpm at the feed rate of 100 mm/min for 8 mm and 10 mm diameter drills of all the drill geometries used in experiments. At very high rpm matrix burning was observed and the fiber did no get cut at a particular angle.

Delamination has been recognized as a major problem that generally regarded as a failure behavior of matrix or resin occurring usually at the interply region. Composite also

poses additional difficulties owing to its inhomogenity and anisotropy. Delamination occurring in unidirectional and multidirectional laminates has been investigated by Jain and Yang [15,16] and the critical thrust values for both cases that causes the onset of delamination were evaluated. A diamond impregnated tubular drill tool for drilling composite laminates was designed and tested that shows little delamination and damage to hole quality. Linear elastic fracture mechanics approach was used to evaluate the expression for the thrust force and empirical formulae in the form of power law describing the thrust force in relation with feed rate and drill diameter relationship were also developed. These relations were combined with critical thrust force expression and a variable feed rate strategically model for drilling in a time optimal fashion was obtained. It was observed that the thrust generated in the multidimensional laminates is lower for any feed that means a higher critical thrust force compared to unidirectional laminates. It was also observed through analysis and experiments that the conventional HSS drill can be use effectively for holes to be drilled are less than quarter of an inch by exploiting the variable feed rate strategy therefore there is need to modify the tool geometry so that the thrust produce can be minimized. The anisotropy of fiber-reinforced plastics heavily influenced the chip formation and cut quality during machining.

Okimichi Yano and Hitoshi Yamaoka [17] discussed about the usefulness of polymers materials in cryo environments. Judgment on the utility of a specific polymer material under cryo condition requires a test demonstration because of the limited data available and uncertain influence of many factors such as sample geometry and the environmental variables. Efforts were also made in the past to overcome drawbacks of

temperature measurement by conventional methods such as use of thermocouple, thermo vision and metallographic techniques which are widely known and commonly employed in the industries. Temperature during machining can also be controlled using micromanipulation technique. In this technique desirable temperature distribution can be achieved (material properties suitable for machining) by applying coolant to selective finite areas. Liu Fei et al [18] and Hong and. Ding [38] developed a 3D dynamic temperature field control models that calculates the temperature of heat sources in the light of tool temperature distribution information. Temperature distribution is analyzed by altering the material properties in each heated sub zone to meet the machinability criteria. Reducing the temperature in those area by providing the coolant increases tool life characteristics and help avoiding the under cooling effect which may increase material strength and cutting resistance and undesirable coolant. Cooling strategies for turning AISI/SAE 1008 includes, cooling the chip below -55^0C, cooling the tool rake face and friction zone to as low temperature as possible and keeping the work piece temperature approximately constant.

Hong and Ding [19] presents a finite element simulation of the cutting temperatures for LN_2 cooled machined processes, a convective heat transfer coefficient is used to evaluate the effects of LN_2 jets on cutting processes estimated experimentally. Two dimensional steady heat transfer finite element model problem was designed with boundary conditions that includes specified temperature, insulated condition and active condition all of which depends upon the coolant jet configurations. The materials used for

machining includes Ti-6Al-V4 and AISI 1008, with varying LN_2 coolant jet configurations and then analyzed using finite element technique.

Turning titanium dry reveals that induced maximum temperature occurs close to cutting edge on the tool chip interface that increases cutting force and provides small tool chip contact length, so dry cutting is not advisable under such circumstances as it leads to unacceptable tool life, especially for high cutting speed. While use of LN_2 minimizes the adhesion and diffusion of the workpiece material to the cutting tool edge maintaining hardness and strength of the tool. The application of the single LN_2 jet, to the tool rake improved the tool life compared to that of conventional emulsion coolants also if in addition to single jet a secondary LN_2 jet was also used that was directed on the tool flank almost doubled the tool life.

While turning AISI 1008 maximum temperature occurred in the secondary deformation zone, poor chip breaking and chip weld at tool rake causing undesirable built up edges. While using LN_2, the thickness of secondary deformation zone was reduced that favors chip breaking. The use of the LN_2 to the tool rake reduced the tool chip interface temperature greatly and decreased the bending resistance of the chip, the use of two LN_2 jets simultaneously to tool rake and chip back allowed the chip to cooled down to embrittlement temperature promoting chip breaking.

Grinding is characterized by high specific energy requirements leading to high grinding zone temperatures and poor surface integrity, Paul and. Chattopadhyay [20, 25, 26] discusses the results that were obtained through experiments with respect to drilling forces, specific energy, grinding zone temperature, and surface residual stress using

cryogenic coolant and compared it with dry grinding and with conventional emulsion cooling. Cryogenic cooling is superior with other coolants in controlling the temperature, residual stresses and grinding forces. The experimental runs were performed on different steels types like mild, high carbon, cold die, hot die and high speed.

For Cryo cooling LN_2 jet was impinged at grinding zone from a distance of 40 mm and at an angle of 20^0 by pressurizing Dewar to 0.35 MPa using dried air and special nozzle. The cryogenic cooling effects on residual stress have been investigated by measuring the residual stress at the ground surface in the direction of grinding by an x-ray diffraction method. The normal and tangential forces and hence specific energy have been found to be less under cryogenic machining for all type of workpiece but as the workpiece hardness increases the benefit of cryogenic cooling decreases for the materials that retains their hardness at high temperature. LN_2 application not only controlled the tensile residual stress but substantially reduced it depending upon material characteristics. With Cryo cooling significant reduction in grinding zone temperature has been observed particularly for ductile material leading to better surface characteristics of ground surface and less wheel loading and wheel wear.

To clarify the interaction mechanism between the drilling tool and work material Caprino and Tagliaferri [21] studied the damage development during drilling of glass polyester composite using standard HSS drill bit and interrupting the process at the preset depths. The feed rate is assumed as a governing parameter for material behavior during drilling. The extent of drill damage was measured by visual inspection at 10 X magnification. The workpiece damage during drilling was located near the exit surface

and is generated when chisel edge emerged from the back face of the panel. For low feed rate there were step like delamination and micro fractures, where as at high feed rates severe damage was observed. The best machining conditions were obtained at a feed rate of 0.024 mm/rev. When the feed rate is too low the damage extent increased slightly due to vibration phenomenon in the workpiece tool system. The degree of delamination is negligible up to 2 mm depth beyond which it increases and reaches maximum near the drill exit edge.

Chandrasekharan et al. [22] developed a model to predict the thrust and torque at the different regions of cutting on a drill for the drilling of CFRP. Their mechanistic approach exploits the geometry of the process, which is independent of the workpiece material. The models were validated independently for the cutting lips and the chisel edge for drilling both metals and fiber-reinforced composite materials for a wide range of machining conditions and drill geometry. Bhatanagar et al. [23] presented some observations made on orthogonal machining of unidirectional carbon fiber reinforced plastics (UD-CFRP) laminates with different fiber orientations. A model for predicting the cutting forces and the dependence of cutting direction on machinability requirements was presented. In their investigation, an approach was developed for modeling the mechanism of chip formation for one broad category of FRP, namely UD-CFRP that showed strong directional dependency. The cutting forces were found to be depending on the fiber angle as well as direction of cutting. The insight into the chip formation mechanism obtained in his work enabled an understanding of the more complex operations such as drilling,

milling, routing where the fiber angle changes with respect to the tool cutting edge continuously.

Wang et al [24, 27, 34] present a technique for machining titanium, tantalum materials along with advanced ceramic composite like reaction bonded silicon nitride 'Si_3N_4' (RBSN), and modern alloys like Inconel. Ceramic composites were machined with Poly Crystalline Boron Nitride tool whereas the rest of them with cemented carbide tool using cryogenic cooling. The system described provide a strong and much stable cooling effect on the insert used, compared to those used in conventional coolants, therefore the temperature effects in the cutting zone was minimized maintaining the higher hot strength and hot hardness of the tool intact and reducing the tool wear. A better surface finish has also been observed using the LN_2 cooling when RBSN was machined without it there was an increase in the flank wear with cutting length. The use of LN_2 increased the tool life allowing the tool to perform well even after extended cutting lengths. There was an increased in the tool life up to five folds when LN_2 coolant was used rather than the conventional coolant. Similar results were obtained when Inconel and Tantalum work materials where machined, without the use of LN_2 there was a sharp increase in temperature in the cutting zone making the tool-workpiece area red hot and formation of built up edges were noticed. But no significant change was observed in the properties of the work material and the cutting forces when LN_2 was used because the cooling was restricted only to the tool without affecting the workpiece material much.

Chou Chen [28] investigated the concept of delamination in drilling CFRP. Delamination is the ratio of the maximum diameter in the damage zone to the hole

diameter. Experiments were performed to investigate the variation of cutting forces with or without onset of delamination during the drilling operations. It was shown that the selection of tool geometry and drilling parameter effects the delamination. An experimental investigation of flank surface temperature is also presented. Experimental results indicated that the flank surface temperature increases with increase in cutting speed but decreasing feed rate. Optimum cutting conditions are proposed to avoid damage from burning during the drilling processes.

Collins [29] presented possible mechanisms and techniques that improve the hardness of the tool and its wear resistance obtained by conventional cold treatment and deep cryo treatment of steels.

Two main processes that occur during heat treatment of steel are transformation of retained austenite and low-temperature conditioning of Martensite. The effects of the cryogenic treatment during the first process includes increase in hardness (the larger the amount of austenite in the microstructure the greater is the increase in hardness), reduction in toughness, improvements in wear resistance, dimensional stability and absence of a secondary hardening peak on the tempering curve following cryogenic treatment. And the effects during the next process includes, much greater number of fine carbide particles in the microstructure, a different partition of alloying elements between matrix and carbides, compared with conventionally treated steels, improvements in wear resistance of the steel, an increase in toughness.

Bhattacharaya & Horrigan, [30] investigated machinability of Kevlar composites by drilling with modified drill bits under cryogenic temperature and compared it with that

of normal drill bits at ambient temperature. It was shown that the KFRP laminates were drilled successfully with HSS drill bits with negative rake and large clearance angles, at commonly available speeds. The average hole surface finish and dimensional quality were found to improved with modified tools. And with the use of cryogenic coolant tool performance was enhanced thereby reducing tool wear rate and hence improved tool life. The problem of KFRP laminates showing fuzzy, uncut and protruding fibres at the entry and exit faces of the holes was minimized to a large extent by using a backing plate made up of thin resin rich layers around the immediate vicinity of the drilling site. It was also noticed that the thrust force generated during drilling at cryogenic temperature or with a modified drill bit is higher than that produced at ambient temperature that builds up the chances of delamination of the composite. But this short comings are weighted against the much improved hole quality and superior tool life.

Fiber arrangements were found more dominant than the often stressed conditions. Pwu and Hocheng [31] showed that fiber angle played the most important role in the mechanism of chip formation and affected the quality of cut for fiber reinforced composite material. Cutting condition showed relatively insignificant influence. He studied analytically and experimentally the chip formation. Bending failure was found to produce chips in cutting perpendicular to fibers. Correlation between the cutting forces, chip thickness and chip length was established.

Hong et al [32] investigated the machining of low carbon steel AISI 1008 a ductile material and reported a significant improvement in chip breaking when the chip is cryogenically cooled. The cooling setup was designed such that the Cryogen is impinged

to the chip faces instead of flooding the whole cutting zone, which optimizes the coolant consumption to a large extent.

Friedrich, [33] examined the specific cutting energy in near-brittle state of Polymethyl Methacrylate in order to estimate the micromilling feed for improved machinability. It was cooled with LN_2, and machined with diamond tools under normal machining conditions. Cutting forces and surface finish were measured from room temperature down to below -53^0C the workpiece material was pre-cooled prior to machining using LN_2. It was found that as the temperature of PMMA was reduced the specific cutting energy increased linearly and the surface finish becomes rougher.

Dhar et al [35] investigated the effects of cryogenic cooling by LN_2 jets on major machinability characteristics in machining C-40 steel, NI-Cr steel by carbide inserts under wide range of cutting speeds and feeds. The coolant in the form of thin high speed jets were impinged through a specially designed nozzle towards the cutting zone along two directions almost parallel to the cutting edges. Effects of tool geometry and effectiveness of LN_2 were also observed. It was noticed that workpiece material characteristics, tool geometry and cutting velocity and feed have significant influence on cryogenic cooling effectiveness. No appreciable changes in chip configuration with cryogenic cooling were noticed but colors of the chips were changed indicating the decrease in temperature and no BUE's. Cryogenic cooling enabled reduction in both thrust and horizontal forces under different feed and speed combinations and for different tool and work combinations. Principal flank wear and auxiliary flank wear decreased substantially for different work tool combinations when cryogenic cooling is employed reflecting the improved tool life.

Surface roughness has been found to be slightly improved by cryogenic cooling. It was concluded that use of cryogenic cooling by liquid nitrogen not only provides friendly environment but also some technological benefits, reduces the cutting forces, tool wear, and dimensional deviation to a large extent and improves the chip formation and surface finish, it provides the benefits mainly through reduction in temperature and favorable change in chip tool interaction, the degree of benefit of this cooling is significantly influenced by the tool geometry, tool work material characteristics and the levels of the machining processes parameters.

Hong and Ding [36, 41] applied LN_2 to cut Ti-6Al-4V, a difficult to machine but widely used material in aerospace industries. Evaluation of cutting temperature obtained under various cooling condition for identifying the effective and economic cooling approach was carried out. They also introduced an innovative and economical dispensing method that directs LN_2 through micro jets to the flank, the rake or both near the cutting edge. Temperatures under cryogenic machining were compared with conventional dry cutting and emulsion coolant machining. Results show that the order of effectiveness of cooling approaches to be (from worst to best) dry cutting, cryogenic tool back cooling, emulsion cooling, pre-cooling the workpiece, cryogenic flank cooling, cryogenic rake cooling and simultaneous rake and flank cooling. In order to maximize the cooling effects the LN_2 must be injected as close as possible to the cutting edge so that points of heat generations can be cooled. They also performed the finite element simulation of temperature distribution during the cryo machining.

Hong and Ding [37] made efforts to overcome drawbacks of temperature measurement by conventional methods such as use of thermocouple, thermo vision and metallographic techniques by making 3D dynamic temperature field control models that calculate the temperature of heat sources in the light of tool temperature distribution information. Temperature during machining can also be controlled using micromanipulation technique. In this technique desirable temperature distribution can be achieved (material properties suitable for machining) by applying coolant to selective finite areas. Temperature distribution is analyzed for altering the material properties in each heated sub zone to meet the machinability criteria. Reducing the temperature in those area by providing the coolant increases tool life characteristics and help avoiding the under cooling effect which may increase material strength and cutting resistance and undesirable coolant. Cooling strategies for turning AISI/SAE 1008 includes, cooling the chip below -55^0C, cooling the tool rake face and friction zone to as low temperature as possible and keeping the work piece temperature approximately constant [9]. Results show reduction in the average auxiliary flank wear during cryogenic cooling, which governs the surface finish and dimensional accuracy of the job.

Dhar et al [38] discussed the role of cryogenic cooling on tool wear and surface finish in plain turning of AISI 1060 steel at industrial speed and feed combinations for two different inserts. They evaluated the effectiveness of cryogenic cooling, compared with the dry and conventional cooling counter parts. The LN_2 jets were impinged using specially designed nozzles along the main cutting and auxiliary cutting edges. The observations showed that dry machining steel cause maximum tool wear and surface

roughness while wet machining didn't show any appreciable improvement. But cryogenic machining using LN_2 provided reduced tool wear, improved tool life and surface finish. The beneficial effects of cooling may also contribute to effective lubrication, retention of tool hardness and favorable chip tool and work tool interaction.

Currently no cryogenic cooling approach exists that is economical and practical enough to replace conventional machining but attempts were made in the past to introduce suitable cryogenic cooling approach that provide minimum wastage of coolant, this can only be done by locating the nozzle at a suitable position that allows proper amount of coolant to be impinged on the desired position during work tool interaction. Hong et al [39] made an effort to find the most effective cryogenic cooling approach that yields the longest tool life while maintaining the minimum usage of LN_2. It is also recommended that the cutting tools shall be cooled not the workpiece material. In order to get optimal cooling the cutting fluid must be applied directly to, and only to, the tip of the cutting tool where the material is being cut and heat is being generated maintaining the flow rate proportional to the heat generated. A micro nozzle is located between the tool face and chip breaker which can be a new economical commercial cutting tool assembly and designed with convenience. During the machining the LN_2 absorbs the heat, evaporates quickly, and forms a fluid cushion between the chip and tool face that functions as lubricant thus reducing the coefficient of friction and secondary deformation. Shane Y. Hong [40] developed a new economical and practical approach to cryogenic machining technique that uses micro nozzle jetting to the cutting point locally minimizing the LN_2 consumption. The work piece materials selected were low and high carbon steels with

titanium and aluminum alloys. The reason that most of the researches selected LN_2 as the cryogen is that, being lighter than air it tends to evaporate and disperse into higher space and has lower boiling point compared to CO_2.

Ugo et al [42] established an approach for the development of damage-free drilling of thermoset laminate composites. Evaluation of the present approach was conducted using Carbon Fiber Reinforced Epoxy (BMS-8-256) composites, frequently used in the aerospace industry. The results of two case studies demonstrate the effectiveness of the new approach in selecting the global optimum drilling parameters for damage free production. In general, high speed and low drilling feed rate are recommended for the production of delamination-free and good surface finish holes in epoxy composites.

By applying high-pressure coolant during machining the tool life and surface finish are found to improve significantly decreasing the heat and cutting forces generated. Senthil et al [43] performed experimental investigation on ASSAB-718 steel material during end milling operation using single uncoated A-30N tungsten carbide insert and a Ti-Al-CN coated insert at a speed of 150 m/min with feed rate of 0.05 mm/tooth and depth of cut 0.35 mm shows the effectiveness of high-pressure coolant in terms of improved surface finish, reduced tool wear and cutting forces, and control of chip shape. The tool wear with high-pressure coolant is significantly better than that with dry cut and conventional coolant. Hence, this reduces the friction at the tool work piece interface and increases the surface finish. Due to high-pressure removal of the heat from the cutting zone cyclic thermal shock does not take place, hence, a lower cutting force can be likely.

Nanda Kishore et al [44, 46] studied cryogenic machining of two types of steels AISI-1040 and AISI-4320 using carbide inserts and concluded that the cooling by LN_2 jets can substantially reduces the cutting forces during machining without affecting the working environment. It also provides benefits mainly by reducing the cutting temperatures, which helps in improving the chip tool interaction and maintains sharpness of the cutting edges.

Reduction in temperature and cutting forces by cryogenic cooling are affected by cutting velocity and feed. Cryogenic cooling becomes more effective when steel rods are machined by SNMM-type inserts which allow the cryogen to reach partially inside or close to the chip tool interface. In machining steels by carbide inserts cryogenic cooling is expected to be more beneficial in finish turning of high strength steels, which are usually done at low feed and cutting velocities.

Dhar et al [45] performed a study on cryogenic machining of plain carbon steels C-40 under varying cutting velocities and feed and concluded that cryogenic cooling if properly employed not only provides the environment safety but also improves machinability characteristics.

Controlling the heat generation is a major problem in high speed machining consequently different techniques are used to estimate the temperature at different locations, since the thermocouple is most widely used technique but it gives us average value of temperature at chip tool interface but not the distribution along the work tool which is very vital for studying the thermal behavior in machining. And for calibration of wide range of temperatures Flame heating technique can be used effectively. As the

cutting zone remains covered by the thick cloud in cryogenic machining modern techniques for measuring the temperatures are not feasible so we can take advantage of numerical techniques, such as 'finite element' that gives us the approximate value.

Earlier research was done using the JEAGER'S model of moving heat sources and block partition principles that doesn't consider the variations in the thermal properties of the work tool material with temperature, elastic-plastic nature of the chip tool interaction, work tool interaction at the wear land in flank but FEM provides the solution for the above mentioned shortcomings of earlier models.

Penetration of cryogen is effective at lower velocity and feed, as large portion of chip tool contact remains elastic nature. A significant improvement of chip breaking can be observed when the chip is cryogenically cooled in the cutting process. Cryogenic embrittlement of the chip also plays a critical role in chip breakability during machining.

Hong et al [47] measured the normal and frictional forces by directly simulating the pure frictional behavior of the tool-chip in cryogenic cutting. A specially designed LN_2 nozzle was used to apply high pressure LN_2 jets through an obstruction type chip breaker in well controlled jets to the tool chip interface, intended to achieve both cooling and lubrication effects with economical LN_2 consumption.

Proper application of LN_2 to the contacting surfaces can reduce frictional coefficients by lowering the interface temperature and modifying the contact pattern that changes sticking contact to purely sliding contact leading to a reduced effective shear strength. It also enhances the hardness of the tool face during cutting maintaining the surface integrity of the harder part, minimizing tendencies of increasing friction. The

lubrication effect of LN_2 can be achieved by combination of various temperature dependent effects and micro scale hydrostatic effects.

A pilot hole is drilled to eliminate the thrust caused by the chisel edge, thus the threat for delamination is significantly reduced Won and Dharan [48] studied the phenomenon of delamination damage produced during the drilling of CFRP and the effect of the chisel edge on the thrust force. They proposed a model that related the delamination of the laminate to drilling parameters and composite properties and also predicts the advantage of a specimen with pre-drilled pilot hole. The diameter of the pre-drilled hole is set equal to the length of chisel edge. The smaller diameter of the pilot hole cannot fully cover the chisel edge, while a larger one tends to cause undesired delamination during pre-drilling. The analysis used a fracture mechanics approach in which the opening mode delamination fracture toughness, a material parameter, was used with a plate model of the laminate. The analysis predicted an optimal thrust force (defined as the minimal thrust force above which delamination is initiated) as a function of drilled hole depth. An advantage of their model was that it could predict varying degrees of delamination for other materials, such as glass fiber-epoxy and for hybrid composites.

Numerous studies have examined the delamination in drilling. Tsao and Hocheng [49] in their research correlated the drill geometry and feed rate to delamination, which leads to severe reduction in the load-carrying capacity of the composite part. The report presents the effects of chisel edge length on delamination and optimal range of pilot hole diameter with chisel edge length is derived. The diameter of the pilot hole is selected equal to chisel length of the drill in order to eliminate the disadvantage of chisel induced

thrust force and avoids the threat of creating a large delamination by large drilled hole. The critical thrust force is a function of material property, uncut thickness and ratio of the chisel edge length to drill diameter for specimens with pre drilled pilot hole. The model presented also explains the usage of pilot hole to assist the quality of drilling of composite material, proper setting of drilling conditions and chisel edge length for delamination free hole have been analyzed. A linear elastic fracture model has been derived analytically that identified the process window of chisel edge length relative to drill diameter for delamination free drilling.

Dini [50] approached the problem of delamination in drilling of GFRP in order to reduce the damage on laminates. A software system is developed and tested with the scope of performing an online prediction of the entity of the damage both at the entry side of the tool and exit side. Feed forward neural networks is used that can give a "measure" of the incipient damage process in function of the cutting conditions like feed rate, tool size, cutting forces, etc. Two architectural of neural networks have also been proposed and investigated to find the best solution in terms of performance, one of the network can sort the predicted delamination in four categories viz. no damage, low, medium and high damage. The other is able to directly predict the average value of the damage. The research also describes the architectural methods of neural network along with the procedure to train and validate them using observation from preliminary drilling tests. The presented neural system has been implemented on a CNC machining centre to obtain a delamination free drilling of GFRP.

Shuaib et al [51] addressed the machinability of plain weave Kevlar 49 composite laminates of different thickness using TiN coated HSS drills. The effect of composite preparation parameters and the drilling conditions on the machinability of the laminates is assessed using the drilling thrust force, cutting torque, and specific cutting energy. The thickness and processing time of the laminates as well as the drilling process parameters were found to influence the maximum value of the thrust force and torque as well as quality of drilled holes. The wear features of the drill used in machining Kevlar composites have found to be different from the conventional wear patterns that occur during drilling metal and alloys.

It has been seen that lot of research has been done in the past to improve the machinability of the difficult to cut materials specially alloys and composite using cryogenic cooling technique. Machining processes like turning and grinding has been widely investigated under cryogenic machining conditions compared to that of drilling. In the present study drilling of aramid fibre composite laminates subjected to low temperature ranges has been investigated for different feed rates and speeds to evaluate the machinability. Also, effects of feed and speed on drilling forces, energy and hole quality for the laminates at low temperature has been studied.

CHAPTER 3

EXPERIMENTAL SETUP AND PROCEDURE

In this chapter, the experimental setup used and the adopted procedure to carry out the investigations is described. This includes the drilling setup used to conduct the experiments, calibration of the dynamometer and the use of PC-based data acquisition system to measure the cutting forces and torque. The cooling techniques implemented to carry out the experiments as well as the drilled hole quality measurements using optical technique are also covered.

3.1 Drilling Setup

Bridgeport series-II N/C milling machine was used for all the drilling experiments described in this research. A schematic diagram and the pictorial view of the experimental setup consisting of the test machine and data acquisition instrumentation are shown in Figure 3.1. The design matrix of the drilling experiments performed at room temperature, 0^0C, -60^0C and -120^0C is shown in Table 3.1. The values of process parameters were selected to correspond to those used by Farhan [56]. A new drill bit was used for each test run. Cryogenic cooling was performed using liquid nitrogen through a special designed fixture which holds the workpiece in place during drilling.

The composite material under investigation was a prepeg plain weave Kevlar 49 composite laminated prepared from Kevlar pre-peg 250^0F type BMS-8-219-285 (1140 denier yarn) with a lay-up of [0/90]. The autoclave pressure and curing temperature were 8 bar and 176^0C respectively. Drilling was performed on 25.4 mm x 320 mm x 2 mm Kevlar 49 composite strip placed on the dynamometer having specially designed fixture to measure the thrust force and torque data during drilling process. The drills used in during the experiments were of high speed steel (HSS) with titanium nitrate (TiN) coating having 6 mm diameter and a point angle of 135^0.

Table 3.1: Test Conditions used for the Drilling Experiments at 20^0C (dry), 0^0C, -60^0C and -120^0C

Test Conditions	Feed Rate (mm/rev)	Speed (rpm)	No. of Holes Drilled
Low Feed Low Speed (f_1N_1)	0.025	1200	60
Low Feed High Speed (f_1N_2)	0.025	3000	60
High Feed Low Speed (f_2N_1)	0.1	1200	60
High Feed High Speed (f_2N_2)	0.1	3000	60

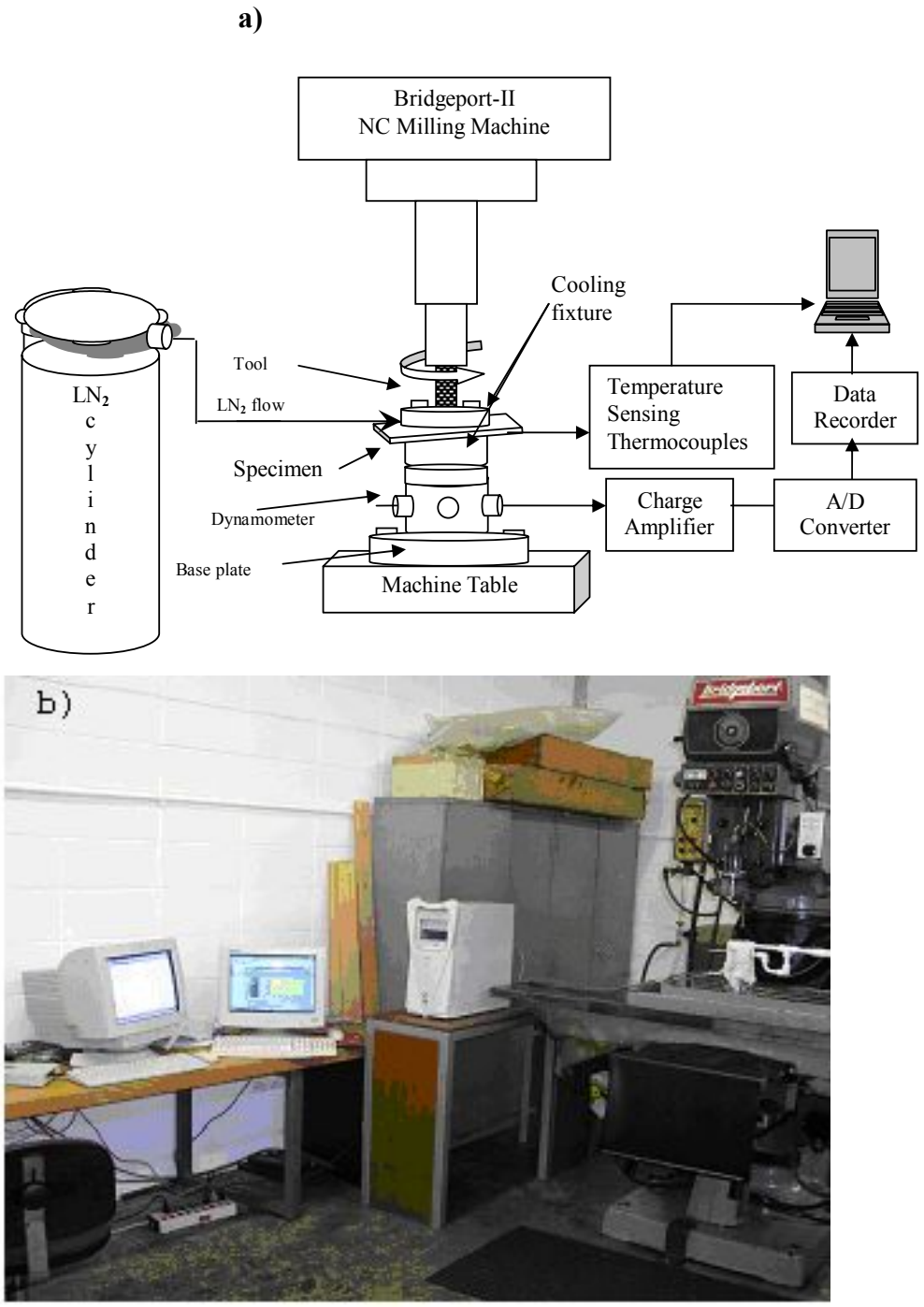

Figure 3.1: a) Schematic Diagram and b) Pictorial View of the Experimental Setup

3.2 Dynamometer Calibration and Data Acquisition System

The dynamometer was calibrated before conducting the drilling test. To obtain the calibration data and calibration curve for the thrust force, Ajax Universal Milling machine fitted with a specially designed fixture shown in Figure 3.2(a) was used. The load was measured by a piezoelectric load cell of CLG-1B type having capacity of 1 ton force manufactured by Tokyo Sokki Kenkyojo Co. Ltd. For the calibration of torque, a specially designed fixture shown in Figure 3.2(b) was used and was mounted on a torque wrench tester model OTT-69-MKG with a capacity of 0 to 500 ft-lb. The calibration was done under ambient laboratory conditions. Humidity, temperature, and pressure recorded at the time of calibration were 41 %, 20.9^0C and 749 mm of Hg. Torque was applied up to 10000 [N-cm] in the interval of 1000 [N-cm]. The calibration data for the dynamometer thrust force and torque are shown in Tables 3.2 and Tables 3.3, respectively whereas the corresponding calibration curves are shown in Figure 3.3 (a) & (b). The drilling thrust force and torque are recorded using a LabView^{TM} based data acquisition system.

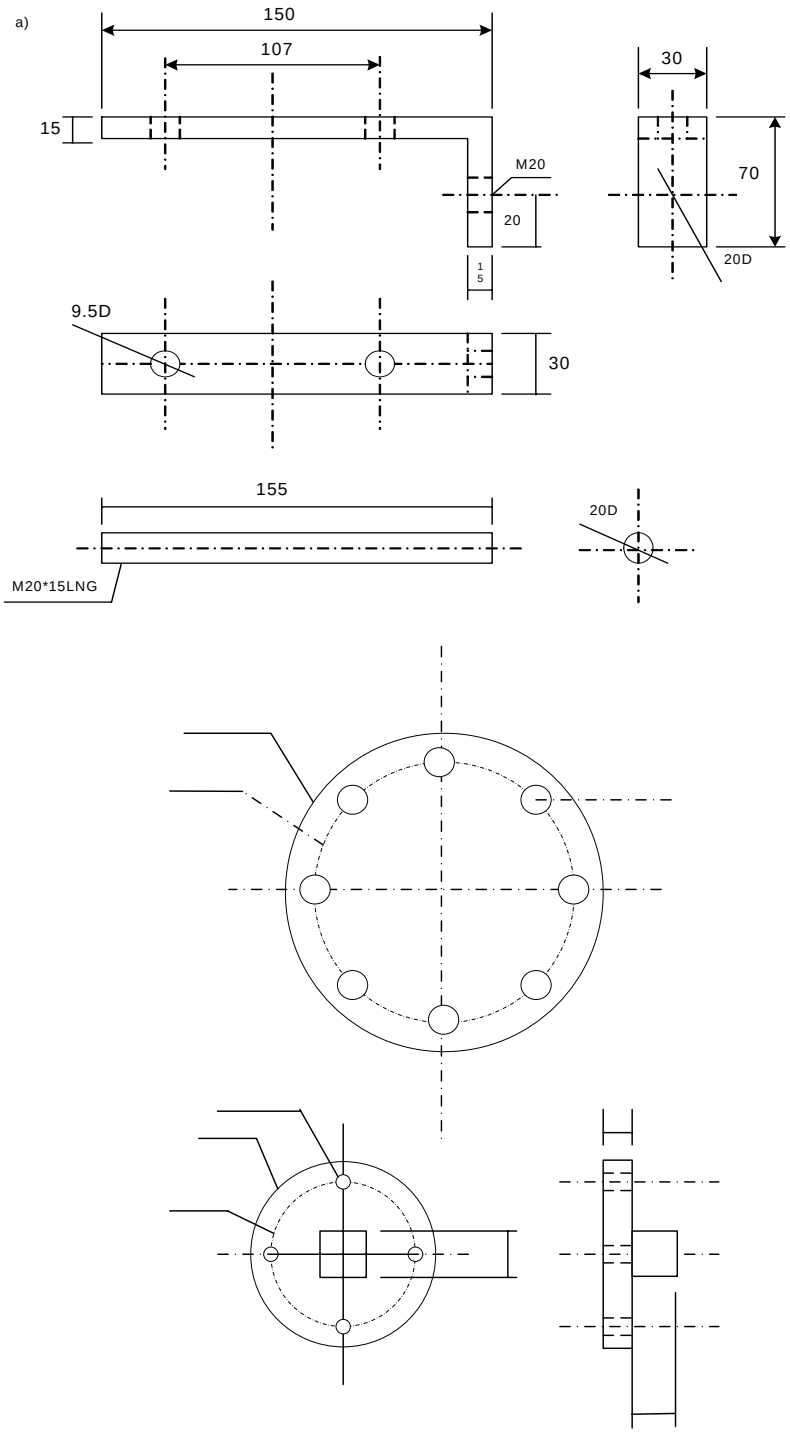

Figure 3.2: Fixtures for Calibration of a) Thrust Force and b) Torque

Table 3.2: Calibration Data for Drilling Thrust Force

Test No.	Applied Load (N)	Instrument Output (pC)
1	0	0.00
2	98.1	12762.25
3	196.2	25524.49
4	294.3	38286.74
5	392.4	51048.98
6	490.5	63811.23
7	588.6	76573.48
8	686.7	89335.72
9	784.8	102097.97
10	882.9	114860.22
11	981	127622.46

Table 3.3: The Calibration Data for Drilling Torque.

Test No.	Applied Torque (N-cm)	InstrumentOutput (pC)
1	0	0.00
2	1000	2430.00
3	2000	4860.00
4	3000	7290.00
5	4000	9720.00
6	5000	12150.00
7	6000	14580.00
8	7000	17010.00
9	8000	19440.00
10	9000	21870.00
11	10000	24300.00

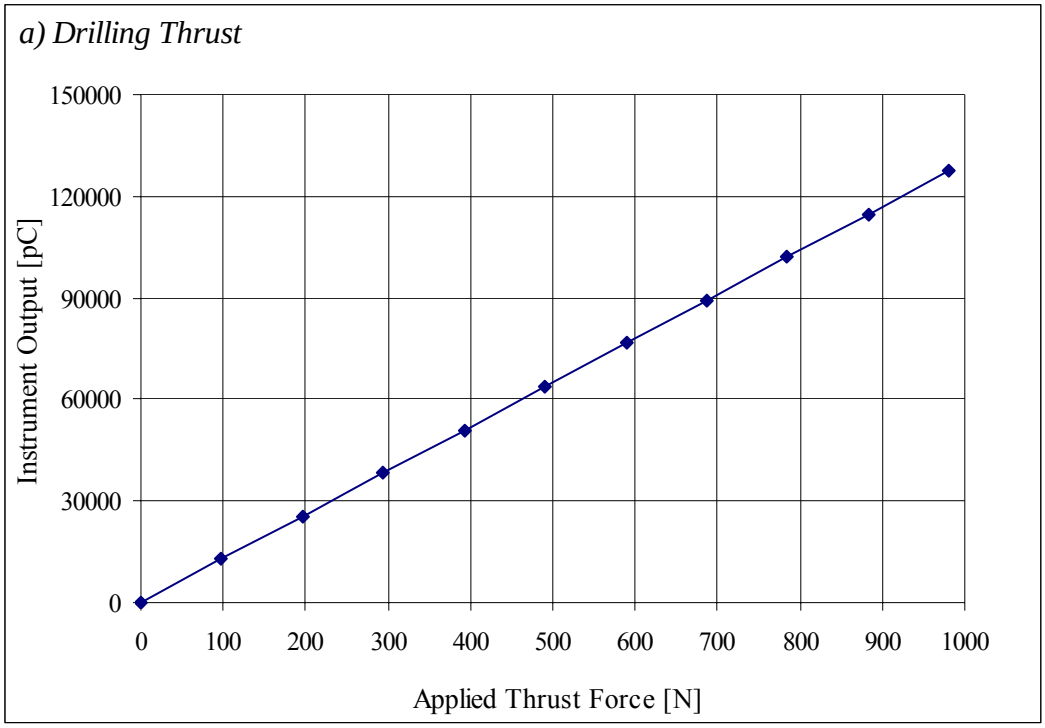

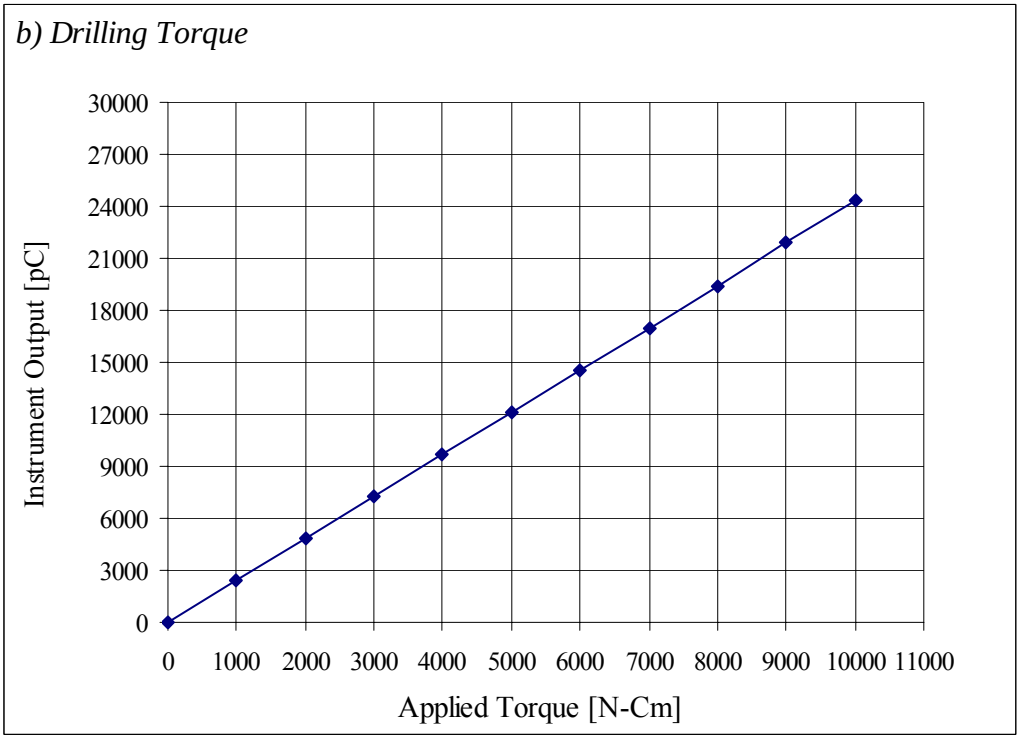

Figure 3.3: Calibration Curves of the Kistler Drilling Dynamometer

3.3 Cooling Technique for Cryo Drilling of the Kevlar Laminates

In order to carry out the drilling in the cryogenic temperature range, liquid nitrogen (LN_2) was used as a coolant. Internal pressure building cylinder of capacity 160 liters filled with liquefied nitrogen gas was used to cool the work piece at the required level of temperatures. A constant flow rate was maintained by opening the cylinder valve up to quarter turn. The fixture is attached to a special tube (hose) for admitting the liquid nitrogen from the cylinder to the workpiece.

In order to measure the temperature of the workpiece T-type Copper-Constantine thermocouples were used. The tip of the thermocouple is inserted at the halfway of the specimen thickness up to a depth of 5 mm in a pre drilled hole as shown in Figure 3.4(a). For each specimen seven thermocouples of length 300 mm, separated by a distance of 40 mm were mounted. The tips were spot welded using a 'TL-WELD' arc spot welding machine shown in Figure 3.4(b) suitable for welding wires up to 1.1 mm (0.043") diameter and have an argon gas shield facility.

The thermocouples were connected using Copper-Constantine connector to measure and record the temperature, the other end of the thermocouple wires are fed into PC using a data interference card. Directview^{TM} software has been used which has an inbuilt program to record the variation of temperature with time. A digital thermometer is also used to monitor the temperature online. The required drilling temperature of the laminate is obtained by opening the LN_2 gas outlet valve and cooling the laminate to a

minimum temperature of -160^{0}C and then the cooling system is shut off to allow the laminates to warm up to the desired drilling temperature of -120^{0}C, -60^{0}C, 0^{0}C and 20^{0}C.

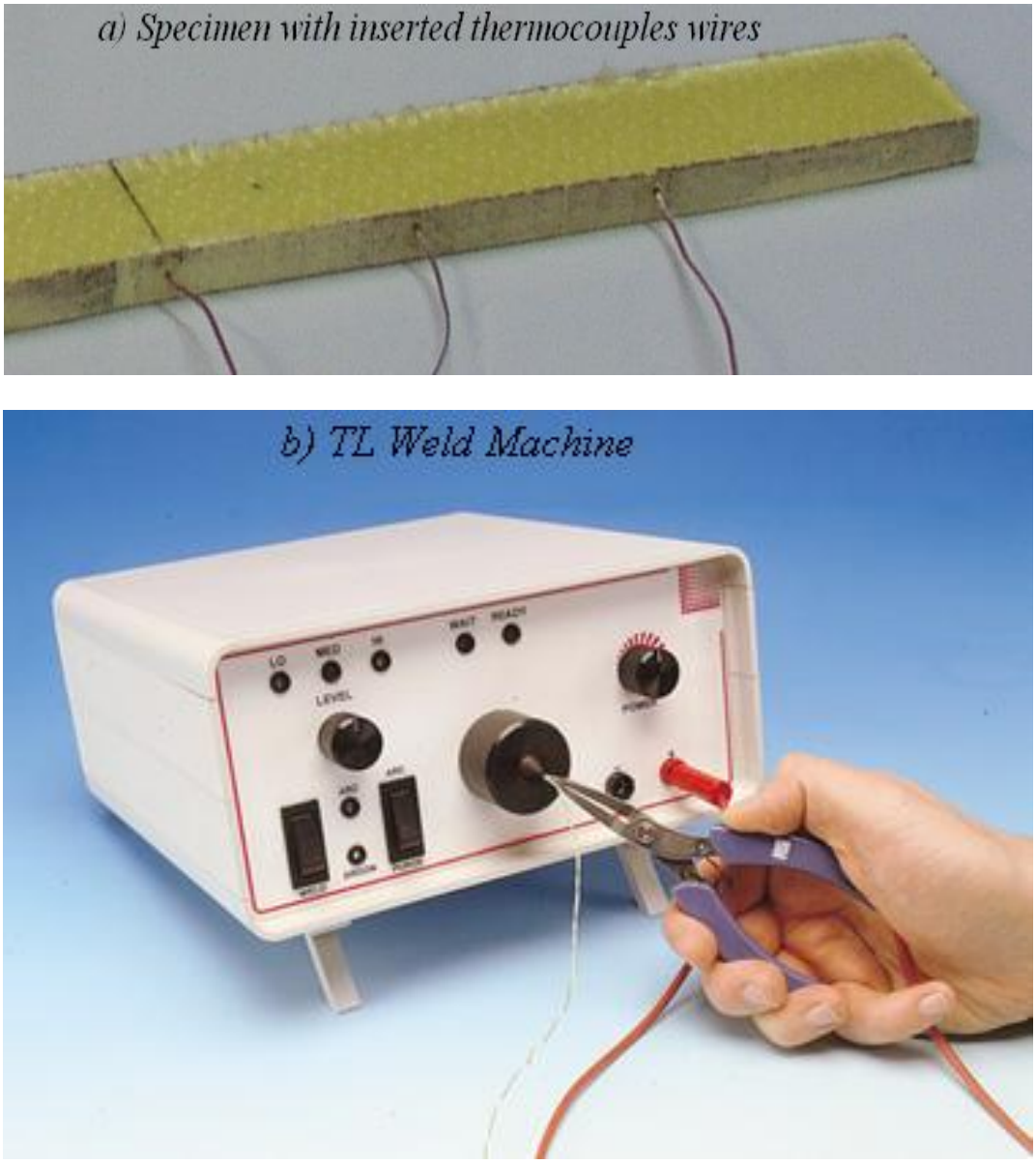

Figure 3.4: a) Specimen with Inserted Thermocouple Wires and b) Thermocouple Welding Machine

3.4 Inspection of Hole Quality using Optical Technique

The surface finish of the drilled holes is an important consideration as AFRP components are often used in applications where fine tolerances are desired. As the drilling operations are usually performed at the end of a production cycle, the hole quality becomes more important with the risk of a part being rejected because of poor tolerance.

In order to check the quality of the holes at various machining conditions and under different workpiece temperatures, holes profiles at the entry and the exit sides have been observed. A high resolution optical microscope has been used for this purpose to provide us the surface pictures of the drilled hole. The scanned pictures of the holes were analyzed using Montivision^{R} Image Analyzer software. A typical hole drilled at high machining conditions at ambient temperature is shown in Figure 3.5. In order to check the extent of the delamination damage during drilling, a parameter called Delamination Factor 'F_d' defined as the ratio of the damaged zone area to the original area has been used as will be detailed in Chapter 5. Surface finish of drilled hole was not used as a machinability criteria, because of the very short length of holes drilled in the 2-mm thick laminates.

Figure 3.5: Damage Zone of the Drilled Hole

CHAPTER 4

RESULTS AND DISCUSSIONS OF DRILLING FORCES & ENERGY

The purpose of the present study is to evaluate the machinability of Aramid composite laminates when drilling at cryogenic temperature levels, using TiN coated drills. The performance evaluation variables are the drilling thrust force, cutting torque, specific cutting energy and the drilled hole quality. The present chapter deals with results pertaining to the effects of cryogenic cooling of Kevlar composite laminates on drilling thrust force, torque and specific energy. The results of tests performed to identify the behavior of the Kevlar-49 composite laminates at cryogenic conditions precede those of the drilling force and torque. These results are used to specify the drilling temperature of the composite laminates.

4.1 Low Temperature Characteristics of Kevlar Laminates

In order to machine the composite laminates at the desired low temperature levels they were first cooled from ambient conditions to the minimum possible temperature while maintaining a constant flow rate of the liquid nitrogen. The coolant flow was then stopped and the laminates were exposed to environment until a desired workpiece temperature is reached for drilling through the laminate. To identify the temperature and

time at which drilling commences a thermocouples wire was inserted at the mid thickness to record the cooling and heating stages of the 25-mm wide Kevlar composite strips through which holes were drilled using TiN coated HSS drills. The attached thermocouple gives the value of temperature of the specimen at the point where the cooling is directed and hole to be drilled. The readings of the thermocouple during the cooling and exposing (environment warming) are plotted against time in Figure 4.1 for the 8-layer laminate. These curves were used to determine the time at which drilling has to start at a certain workpiece temperature.

To predict when to start drilling at a desired temperature, after starting the cooling cycle, the time taken to cool the laminate to its minimum temperature level (-160^0C) is added to that used in exposing it to environment till the desired drilling temperature. The total time "t_t" for the specimen to reach the specified machining temperature is given by:

$$t_t = t_c + t_w$$

Where "t_c" = time taken to reach the lowest possible temperature (i.e. -160^0C) and

"t_w" = time for warming up of the specimen to the machining temperature

The temperature 'T' versus 't_w' time of exposure from minimum temperature to the drilling temperature of the laminate was found to be represented by an exponential function $T = T_m \exp(\alpha t_w)$, where 'T_m' is the minimum temperature to which the laminate is cooled, 'α' is the time constant. This function can predict very well the temperature values from lowest temperature till 0^0C. The temperature profile recorded by the thermocouple which is located at the drilled hole position for the 8-layer laminate,

resulted in T_m = -129.8 ^{0}C and α = -0.0051. The plot of the raw data and the model are shown in Figure 4.2. The time 't_w' for exposure of the specimen, after reaching its minimum temperature and shutting off the coolant, to a desired workpiece temperature for drilling was calculated using the following equation

$$t_w = \frac{1}{\alpha} \ln\left(\frac{T}{T_m}\right)$$

Where 'T' is the desired machining temperature, 'α' and 'T_m' are the temperature model constants respectively. The time required for the 8-layer laminate to reach the drilling temperatures 0^{0}C, -60^{0}C, and –120^{0}C are listed in Table 4.1 below. These values are in agreement with those mentioned by Bhattacharaya et al (11).

Table 4.1 Specimen Exposure Time in Reaching the Required Drilling Temperature

MODEL CONSTANTS		DRILLING TEMPERATURE T(^{0}C)	TIME 'T_W' (SECS)
T_M	α		
-129.8	-0.0051	0	1100
		-60	151
		-120	15

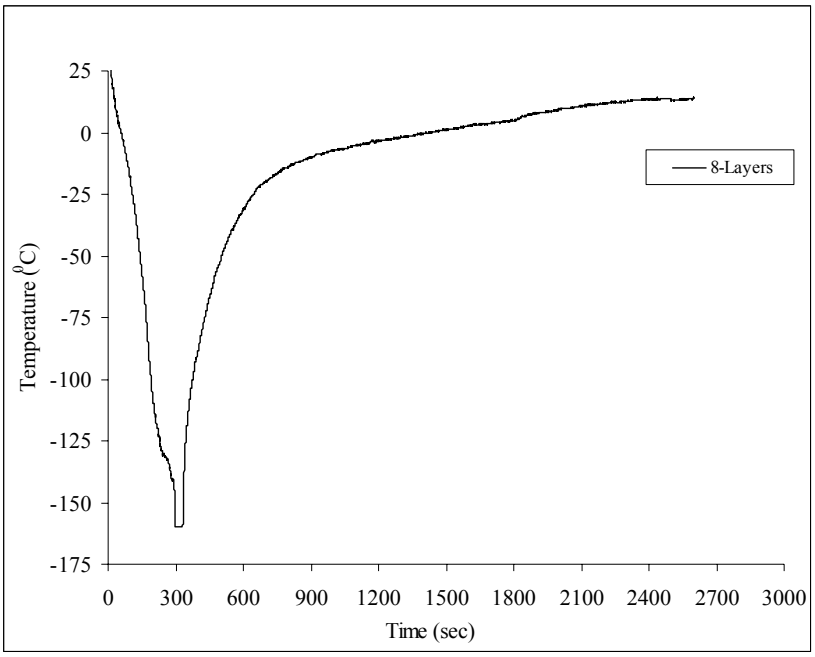

Figure 4.1: Temperature Variations of Kevlar Laminate Having 8 Layers

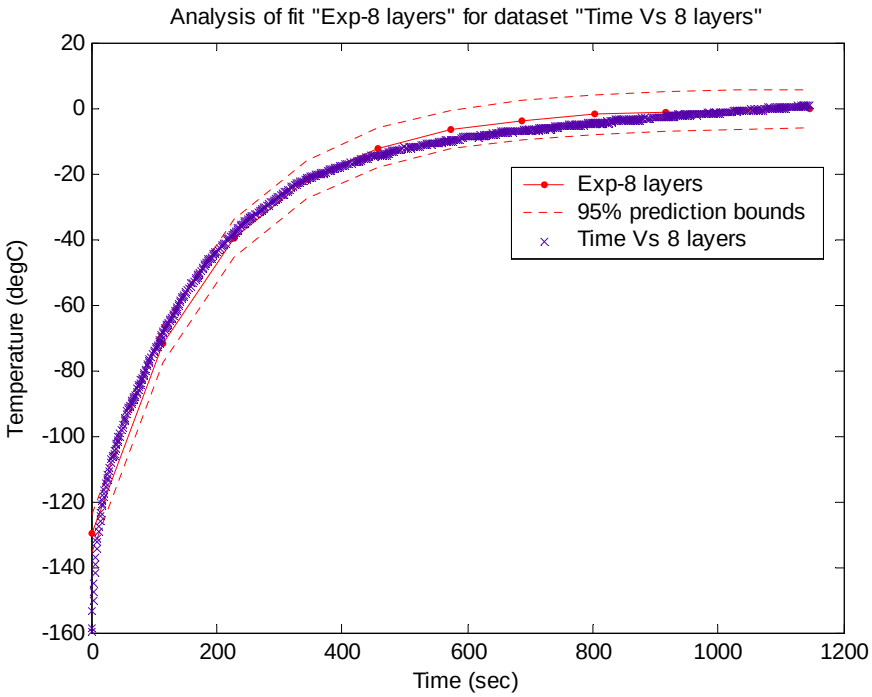

Figure 4.2: Fitted Curve during Exposure of the Kevlar Composite Laminates having 8 Layers

4.2 Effect of Low Temperature on Drilling Forces and Energy

The experimental raw data of the force and torque were filtered first using Matlab^{TM} 6.5 to remove the background noise. Figure 4.3(a) shows a typical measurement of thrust force raw data at f=0.1 mm/rev and N=3000 rpm machining condition, plotted with respect to the hole depth (machining time) at a sampling rate of 1000 cycles/sec, while Figure 4.3(b) shows the filtered plot of the same. The variations are similar to that described by Jain et al [15] and Tsao et al [49] for drilling of fibre reinforced composites. DiIlio et al [7] mentioned that the peaks of thrust force during cutting of composite materials depend on the inhomogenity of the material and the interface between the laminates. The procedure of the data filtering is summarized in the Appendix-A.

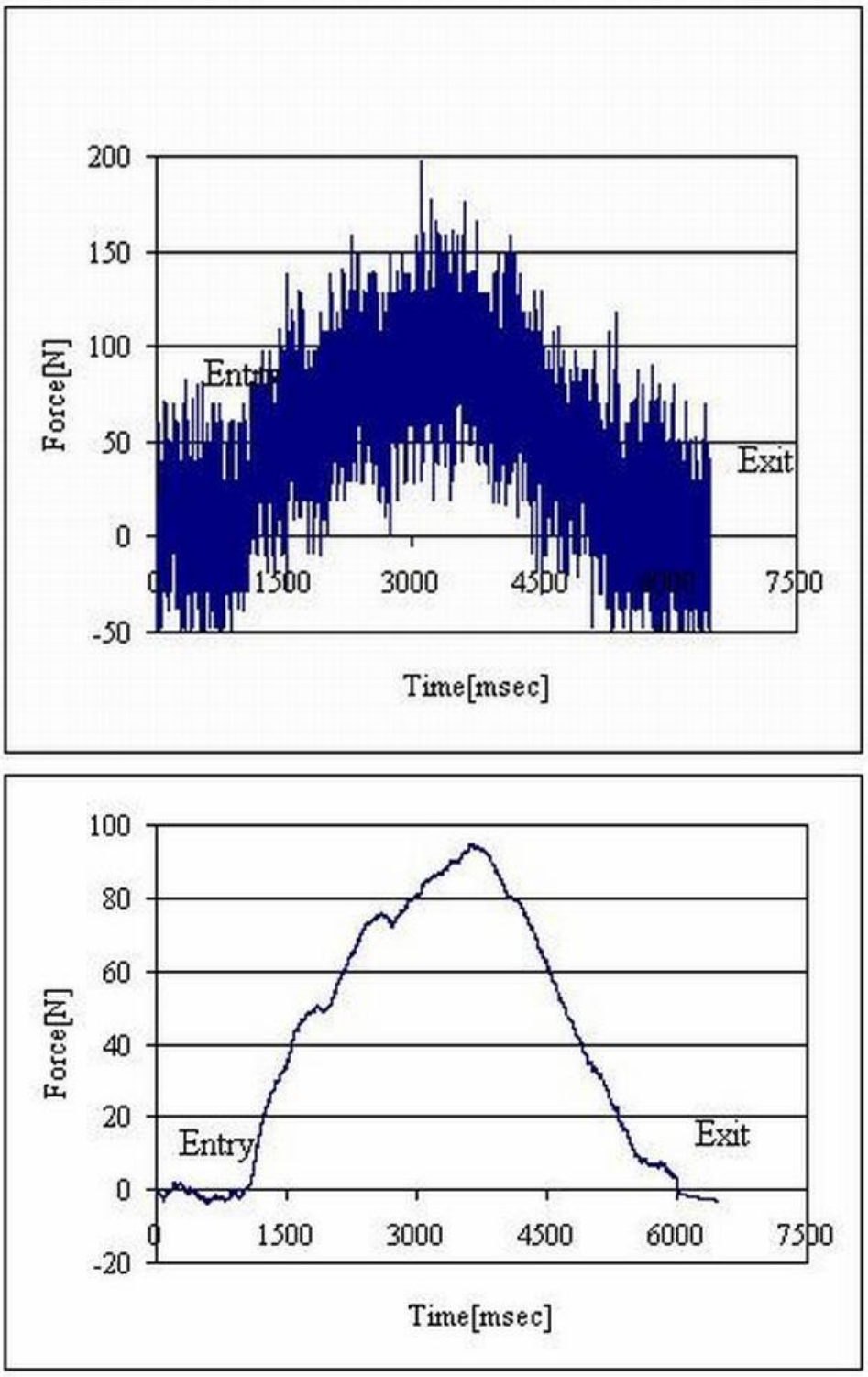

Figure 4.3: Signals of a) Raw and b) Filtered Force Data during Drilling a Hole

Table 4.2 to Tables 4.5 contain the maximum thrust force and torque data of the Kevlar composite laminates at 20^0C (dry), 0^0C, -60^0C and -120^0C and drilled at each of the four test conditions. The tables also include in the second column the machining time for the number of holes drilled at a certain cutting conditions obtained by dividing the distance traveled axially by the drill by its feed speed. The data in these tables will be used to evaluate the effects of workpiece temperature, cutting speed and feed rate on the maximum drilling forces of the Kevlar composite laminate. Typical variation of thrust force and torque with the number of holes when drilling with feed = 0.025 mm/rev and speed = 1200 rpm is shown in Figure 4.5 and Figure 4.6 for the four workpiece temperatures. All thrust force and torque data exhibited similar variation.

Visual inspection of the drilling thrust force and torque variation with the number of holes drilled reveal the fact that for all test conditions of the Kevlar composite laminates, they fluctuate around a certain average value and do not reveal the known increasing trend which characterizes the force behavior when machining metals and alloys. The observed variations of the drilling thrust and torque follow the results reported by Shuaib et al (51) and Farhan Hamid (56) who used random variable to express the apparent stochastic variation. Following the same approach of these authors, adequate statistical probability distribution models were fitted to the drilling thrust force and torque data sets, using Chi-square (chi-sq) and Kolmogrov-Smirnov (K-S) goodness of fit tests, implemented via Statistica™ software. The normal probability distribution has been found to be the adequate distribution model for all data sets of Kevlar composite laminates.

It is difficult to draw comprehensible conclusions about the effect of workpiece temperature, speed and feed rate on the drilling thrust and torque of the Kevlar laminates by visual inspection of the plots in Figure 4.5 and Figure 4.6 alone because of the high degree of overlap between the data sets in these figures. We therefore resort to statistical approaches, namely test of hypothesis (See Appendix-B), to evaluate the effect of these parameters on the drilling thrust force and torque. This is achieved by using statistical inferences to compare the respective estimated statistical parameters (mean and standard deviation) of the adequate normal probability models listed in Table 4.6 and Table 4.7 for the thrust force and torque, respectively.

Table 4.2: Thrust Force and Torque Data when Drilling at Different Workpiece Temperatures with Feed = 0.025 mm/rev and Speed = 1200 rpm

		Ambient (20°C)		0°C		-60°C		-120°C	
Hole No.	Machining Time (sec)	"F_z" Max (N)	"M_z" Max (N-cm)	"F_z" Max (N)	"M_z" Max (N-cm)	"F_z" Max (N)	"M_z" Max (N-cm)	"F_z" Max (N)	"M_z" Max (N-cm)
1	4	108.939	2.503	104.241	7.263	151.425	38.175	185.766	80.525
2	8	104.250	0.989	125.328	13.306	151.425	62.328	198.831	59.974
3	12	104.250	3.850	107.997	13.306	151.425	21.983	205.266	80.525
4	16	110.262	1.614	97.557	17.326	151.425	57.506	216.246	53.449
5	20	110.262	5.839	102.279	21.122	151.425	57.406	192.516	64.351
6	24	116.766	3.636	97.308	22.273	151.425	58.397	183.198	65.780
7	28	110.297	4.524	88.593	22.677	151.425	52.414	216.000	55.945
8	32	110.004	2.585	98.067	22.677	151.425	44.823	222.819	56.599
9	36	103.430	7.365	99.024	25.796	149.634	64.910	196.452	87.372
10	40	127.536	7.004	95.298	25.796	149.634	21.185	198.585	88.869
11	44	108.315	3.945	96.597	20.265	167.364	47.135	211.020	62.757
12	48	113.391	3.566	101.127	24.270	175.395	66.491	208.314	83.629
13	52	113.391	6.767	105.762	24.270	175.395	62.055	214.173	71.248
14	56	93.551	6.532	98.757	22.972	162.822	36.220	191.778	52.072
15	60	60.762	10.207	103.080	23.744	158.178	54.203	217.806	73.662
16	64	92.262	2.529	99.546	24.605	164.553	60.213	196.278	83.909
17	68	99.948	2.644	110.322	20.075	155.586	59.324	210.681	82.452
18	72	123.270	3.807	102.729	20.075	155.586	67.737	217.476	87.118
19	76	97.911	3.030	103.713	20.075	155.586	62.786	216.294	74.352
20	80	107.602	6.193	99.351	18.042	158.223	63.623	209.601	62.342
21	84	77.040	6.001	96.831	23.034	178.677	67.791	210.798	59.438
22	88	85.011	8.198	98.874	23.034	178.677	61.272	202.548	59.607
23	92	83.154	6.575	119.883	20.931	165.846	55.856	168.198	59.804
24	96	83.703	4.165	154.101	20.162	165.402	63.857	205.980	78.859
25	100	126.891	4.860	112.149	20.162	165.402	30.017	199.581	73.542
26	104	109.419	5.839	115.230	17.319	161.697	46.136	204.399	53.123
27	108	107.590	3.636	122.571	29.150	176.499	48.843	210.681	71.556
28	112	84.210	4.524	134.517	29.150	176.499	36.126	217.476	97.186
29	116	80.670	2.585	136.863	19.602	170.589	22.365	216.294	78.533
30	120	138.972	10.715	132.081	23.991	160.992	40.100	209.601	83.223

(Cont…) Table 4.2

		Ambient (20°C)		0°C		-60°C		-120°C	
Hole No.	Machining Time (sec)	"F_z" Max (N)	"M_z" Max (N-cm)	"F_z" Max (N)	"M_z" Max (N-cm)	"F_z" Max (N)	"M_z" Max (N-cm)	"F_z" Max (N)	"M_z" Max (N-cm)
31	124	98.577	9.684	110.079	23.991	160.992	47.711	205.980	107.874
32	128	100.477	3.945	127.590	17.501	159.177	60.045	199.581	96.319
33	132	51.645	3.566	118.707	17.541	163.080	58.203	204.399	49.361
34	136	84.753	6.767	107.793	17.541	163.080	52.615	210.681	84.889
35	140	92.297	6.532	166.509	18.588	164.178	48.267	217.476	57.804
36	144	72.165	10.207	154.101	20.261	168.018	63.623	216.294	54.220
37	148	69.315	12.893	112.149	20.036	169.005	67.791	209.601	48.294
38	152	108.012	6.001	115.230	18.160	165.171	61.272	210.798	74.423
39	156	95.304	8.198	122.571	17.271	165.048	55.856	196.452	58.575
40	160	98.025	6.575	134.517	17.271	165.048	63.857	198.585	67.193
41	164	94.407	10.865	136.863	28.266	163.494	30.017	211.020	75.237
42	168	108.759	4.860	132.081	28.266	163.494	46.136	208.314	48.363
43	172	102.120	5.839	110.079	15.140	159.372	48.843	214.173	48.495
44	176	115.278	3.636	127.590	15.140	159.372	30.017	191.778	57.804
45	180	134.319	4.524	118.707	21.873	163.326	46.136	217.806	54.220
46	184	136.032	2.585	107.793	17.374	168.414	48.843	196.278	48.294
47	188	105.036	10.715	166.509	22.602	163.311	36.126	210.681	74.423
48	192	133.266	9.684	154.101	22.602	163.311	22.365	196.278	53.123
49	196	152.367	3.566	112.149	14.149	160.227	40.100	210.681	71.556
50	200	103.430	6.767	115.230	17.341	163.923	47.711	217.476	97.186
51	204	127.536	6.532	122.571	17.341	163.923	64.910	216.294	78.533
52	208	108.315	10.207	134.517	23.839	166.563	21.185	209.601	83.223
53	212	113.391	12.893	136.863	23.839	166.563	47.135	210.798	56.599
54	216	113.391	6.001	118.707	24.550	160.986	66.491	202.548	87.372
55	220	93.551	8.198	107.793	22.002	167.973	62.055	168.198	88.869
56	224	60.762	3.636	166.509	18.132	165.714	36.220	210.681	62.757
57	228	92.262	4.524	154.101	18.132	165.714	54.203	196.278	83.629
58	232	99.948	2.585	112.149	17.102	163.953	60.213	210.681	71.248
59	236	123.270	10.715	115.230	18.288	166.089	66.491	217.476	52.072
60	240	97.911	10.715	122.571	19.974	165.213	62.055	196.278	88.869

Table 4.3: Thrust Force and Torque Data when Drilling at Different Workpiece Temperatures with feed = 0.025 mm/rev and speed = 3000 rpm

		Ambient (20°C)		0°C		-60°C		-120°C	
Hole No.	Machining Time (sec)	"F_z" Max (N)	"M_z" Max (N-cm)	"F_z" Max (N)	"M_z" Max (N-cm)	"F_z" Max (N)	"M_z" Max (N-cm)	"F_z" Max (N)	"M_z" Max (N-cm)
1	1.6	110.406	5.329	103.989	24.097	150.930	11.858	164.508	15.094
2	3.2	102.561	4.666	106.380	9.631	154.044	7.819	174.984	64.047
3	4.8	74.184	9.243	117.000	2.996	154.884	8.735	186.468	62.030
4	6.4	93.651	4.450	117.000	4.556	166.146	8.735	211.008	65.818
5	8	97.119	9.097	94.527	9.615	140.688	10.594	181.254	43.860
6	9.6	75.624	12.209	90.351	10.492	140.529	12.759	199.278	34.296
7	11.2	41.085	6.607	94.782	3.881	156.399	13.062	193.230	33.667
8	12.8	85.809	3.675	91.851	5.333	146.676	9.377	169.887	35.868
9	14.4	51.489	10.526	91.851	3.340	161.499	9.377	190.149	46.619
10	16	114.249	0.795	91.020	7.477	152.610	12.663	175.407	8.403
11	17.6	41.631	11.778	91.020	4.707	151.110	12.663	191.238	46.163
12	19.2	59.826	5.183	117.567	10.743	174.345	18.169	166.629	28.823
13	20.8	114.327	5.191	90.228	7.755	159.297	19.441	171.585	39.718
14	22.4	54.711	9.848	93.960	8.926	140.778	25.011	175.323	46.525
15	24	37.251	13.164	91.869	17.388	181.674	23.283	157.278	34.936
16	25.6	55.998	6.807	91.869	15.996	206.946	29.983	168.129	51.670
17	27.2	40.467	4.609	92.724	3.370	144.372	23.557	156.363	48.789
18	28.8	110.817	6.010	95.781	14.967	159.189	28.467	142.935	9.308
19	30.4	72.705	1.724	97.911	5.114	142.809	23.012	159.762	34.413
20	32	42.765	14.219	97.911	10.352	149.025	29.712	176.190	29.454
21	33.6	47.142	3.474	93.900	12.532	157.527	34.512	192.867	28.198
22	35.2	56.391	4.289	91.113	17.785	147.105	18.460	195.375	23.807
23	36.8	56.991	5.477	94.689	5.358	162.825	14.173	207.984	17.129
24	38.4	37.398	4.865	93.333	12.930	120.570	8.767	173.907	23.092
25	40	46.167	8.412	94.173	4.348	145.197	12.620	170.823	33.211
26	41.6	100.461	0.795	91.389	7.309	178.104	11.661	192.702	29.455
27	43.2	55.368	11.778	95.442	8.637	173.319	10.640	192.927	31.234
28	44.8	81.027	5.183	95.442	11.771	151.371	10.640	187.758	35.016
29	46.4	40.872	5.191	96.744	23.979	154.956	9.212	174.540	29.677
30	48	42.630	9.848	96.744	9.636	131.532	9.212	179.649	31.153

(Cont…) Table 4.3

		Ambient (20°C)		0°C		-60°C		-120°C	
Hole No.	Machining Time (sec)	"F_z" Max (N)	"M_z" Max (N-cm)	"F_z" Max (N)	"M_z" Max (N-cm)	"F_z" Max (N)	"M_z" Max (N-cm)	"F_z" Max (N)	"M_z" Max (N-cm)
31	49.6	57.199	13.164	93.342	5.217	153.894	25.497	185.157	30.048
32	51.2	87.222	6.807	95.394	15.417	155.685	16.854	190.161	31.849
33	52.8	105.921	4.609	89.187	7.381	181.455	9.263	196.161	30.929
34	54.4	123.303	6.010	93.471	8.940	171.957	12.660	189.810	31.177
35	56	42.531	1.724	94.887	14.294	144.936	10.731	175.323	56.612
36	57.6	93.951	7.519	98.283	4.383	143.337	9.456	157.278	31.377
37	59.2	119.352	3.474	96.357	12.930	162.825	7.473	168.129	31.697
38	60.8	114.000	9.848	95.445	4.348	120.570	24.378	156.363	30.718
39	62.4	45.903	13.164	94.059	7.309	145.197	24.378	142.935	31.028
40	64	44.286	6.807	95.292	8.637	178.104	15.910	159.762	39.844
41	65.6	81.999	4.609	101.775	11.771	173.319	16.399	176.190	28.446
42	67.2	100.065	6.010	92.553	23.979	151.371	22.800	192.867	30.298
43	68.8	120.846	1.724	98.268	9.636	154.956	8.425	195.375	38.340
44	70.4	118.239	14.219	100.317	5.217	131.532	14.409	207.984	28.669
45	72	94.971	3.474	102.438	15.417	153.894	16.684	173.907	46.317
46	73.6	118.101	4.289	105.753	15.417	155.685	15.039	170.823	28.495
47	75.2	125.886	5.477	98.886	7.381	181.455	15.762	192.927	56.612
48	76.8	64.341	4.865	97.263	8.940	171.957	13.565	187.758	31.377
49	78.4	55.002	8.412	97.665	17.388	144.936	17.990	174.540	31.697
50	80	79.362	0.795	96.564	15.996	143.337	15.515	179.649	30.718
51	81.6	57.192	11.778	97.653	3.370	162.825	15.033	185.157	31.028
52	83.2	118.239	6.010	101.991	14.967	151.371	12.394	190.161	39.844
53	84.8	94.971	1.724	107.609	5.114	154.956	12.512	196.161	30.718
54	86.4	118.101	20.919	106.062	10.352	131.532	31.728	189.810	31.028
55	88	125.886	3.474	103.281	12.532	153.894	24.023	175.323	39.844
56	89.6	81.999	9.848	103.413	17.785	162.825	7.937	157.278	31.153
57	91.2	100.065	13.164	97.533	5.358	151.371	16.564	168.129	30.048
58	92.8	120.846	6.807	96.933	12.930	131.532	29.996	190.161	31.849
59	94.4	118.239	4.609	96.837	4.348	153.894	12.706	196.161	30.929
60	96	94.971	4.865	101.127	7.309	162.825	15.256	189.810	31.177

Table 4.4: Thrust Force and Torque Data when Drilling at Different Workpiece Temperatures with feed = 0.1 mm/rev and speed = 1200 rpm

		Ambient (20°C)		0°C		-60°C		-120°C	
Hole No.	Machining Time (sec)	"F_z" Max (N)	"M_z" Max (N-cm)	"F_z" Max (N)	"M_z" Max (N-cm)	"F_z" Max (N)	"M_z" Max (N-cm)	"F_z" Max (N)	"M_z" Max (N-cm)
1	1	135.000	9.876	83.619	9.588	159.798	9.703	226.704	2.518
2	2	150.000	13.693	131.895	31.318	227.850	7.450	231.279	12.447
3	3	165.000	10.646	135.870	26.064	155.910	7.962	244.416	0.000
4	4	180.387	11.580	125.037	20.851	203.733	16.157	240.327	20.280
5	5	174.168	10.359	136.302	22.351	177.459	14.899	320.880	41.406
6	6	184.959	11.691	133.749	10.572	221.757	15.530	244.248	19.002
7	7	189.909	9.911	137.241	12.460	209.640	9.856	249.297	34.598
8	8	177.849	13.907	134.832	19.782	185.883	14.418	237.732	23.756
9	9	175.524	8.656	139.164	11.418	181.935	15.781	283.422	49.532
10	10	180.321	7.529	141.306	12.174	216.030	31.345	243.558	41.689
11	11	177.660	22.524	134.985	11.316	182.364	17.403	282.678	36.113
12	12	189.687	8.622	195.171	13.677	177.543	27.509	264.201	33.846
13	13	180.414	10.618	142.281	16.132	178.920	23.138	276.114	38.857
14	14	183.171	13.359	240.183	20.479	172.080	36.807	313.200	61.943
15	15	188.325	11.988	208.950	13.538	169.488	30.687	235.077	22.503
16	16	180.462	12.028	153.225	24.222	201.645	31.647	242.295	19.334
17	17	187.776	8.528	131.370	21.534	168.825	22.455	262.917	22.961
18	18	180.195	8.697	121.506	25.226	197.997	9.217	286.893	29.636
19	19	192.954	6.774	181.245	13.400	170.550	33.137	270.000	22.324
20	20	173.415	19.669	130.986	13.309	191.799	34.100	257.304	27.659
21	21	165.000	11.544	131.268	26.578	176.799	24.129	312.570	35.494
22	22	196.161	12.605	153.699	13.400	171.066	19.705	270.000	32.890
23	23	208.665	7.283	145.356	17.309	188.385	29.721	321.120	28.408
24	24	189.273	9.434	175.740	15.330	208.278	39.222	251.142	8.638
25	25	197.877	11.790	191.349	12.828	151.902	27.376	288.135	8.056
26	26	198.513	11.550	150.801	22.838	166.413	21.889	285.747	9.019
27	27	193.050	10.713	165.888	6.857	175.521	30.385	310.110	4.970
28	28	198.963	13.234	159.417	22.013	177.159	12.898	325.710	8.088
29	29	205.836	11.399	164.550	27.478	170.988	13.480	325.410	4.698
30	30	204.471	9.429	155.181	12.627	190.755	17.139	343.170	28.750

(Cont…) Table 4.4

		Ambient (20°C)		0°C		-60°C		-120°C	
Hole No.	Machining Time (sec)	"F_z" Max (N)	"M_z" Max (N-cm)	"F_z" Max (N)	"M_z" Max (N-cm)	"F_z" Max (N)	"M_z" Max (N-cm)	"F_z" Max (N)	"M_z" Max (N-cm)
31	31	209.199	10.674	193.110	13.011	179.859	15.913	328.260	32.809
32	32	193.785	8.709	175.182	21.051	182.025	13.507	302.640	24.888
33	33	210.087	13.675	163.455	13.653	167.409	19.631	343.590	8.360
34	34	205.902	21.130	181.617	14.695	181.485	9.514	339.360	40.943
35	35	215.067	18.733	183.243	13.199	162.954	13.983	315.840	35.237
36	36	200.340	12.417	172.038	5.337	170.550	21.534	299.793	52.119
37	37	193.416	13.393	183.285	13.538	191.799	10.934	310.110	50.377
38	38	226.413	10.598	183.945	24.222	176.799	22.077	325.710	50.009
39	39	204.714	9.429	183.993	21.534	171.066	22.211	325.410	34.537
40	40	236.379	10.674	180.462	25.226	188.385	36.669	343.170	35.369
41	41	201.792	8.709	185.007	13.400	208.278	9.514	343.590	58.240
42	42	203.328	13.675	155.160	13.309	151.902	19.705	339.360	29.974
43	43	183.759	21.130	180.222	26.578	166.413	29.721	315.840	58.223
44	44	188.523	18.733	179.409	13.400	175.521	39.222	325.710	12.567
45	45	196.473	12.417	254.352	17.309	177.159	20.676	325.410	31.065
46	46	187.200	13.393	208.998	15.330	170.988	21.889	343.170	57.044
47	47	191.688	10.598	153.246	16.132	190.755	21.889	328.260	21.246
48	48	198.552	11.550	195.405	20.479	179.859	28.589	302.640	14.599
49	49	209.436	10.713	200.730	13.538	182.025	13.480	343.590	20.308
50	50	204.660	13.234	196.407	24.222	167.409	17.139	339.360	22.180
51	51	191.148	11.399	171.759	21.534	181.485	15.913	321.120	26.348
52	52	195.744	9.429	185.007	25.226	162.954	13.507	251.142	22.758
53	53	205.191	21.130	155.160	13.400	170.550	19.631	288.135	29.704
54	54	192.012	18.733	180.222	13.309	191.799	9.514	285.747	13.294
55	55	202.356	12.417	179.409	26.578	176.799	13.983	310.110	42.483
56	56	196.401	13.393	254.352	13.400	171.066	21.534	325.710	66.973
57	57	193.350	10.598	208.998	17.309	188.385	10.934	288.135	72.950
58	58	205.239	11.550	153.246	15.330	208.278	22.077	285.747	71.563
59	59	193.566	10.713	195.405	21.534	151.902	22.211	310.110	53.565
60	60	187.860	13.234	254.352	25.226	190.755	36.669	328.260	0.000

Table 4.5: Thrust Force and Torque Data when Drilling at Different Workpiece Temperatures with feed = 0.1 mm/rev and speed = 3000 rpm

		Ambient (20°C)		0°C		-60°C		-120°C	
Hole No.	Machining Time (sec)	"F_z" Max (N)	"M_z" Max (N-cm)	"F_z" Max (N)	"M_z" Max (N-cm)	"F_z" Max (N)	"M_z" Max (N-cm)	"F_z" Max (N)	"M_z" Max (N-cm)
1	0.4	108.366	7.665	124.698	3.668	185.178	8.643	239.976	28.477
2	0.8	82.857	9.802	111.681	11.415	168.321	10.184	264.276	28.555
3	1.2	106.086	9.673	116.052	9.338	209.358	12.194	198.765	32.723
4	1.6	106.017	8.715	97.581	21.293	172.224	17.487	214.122	38.511
5	2	99.276	7.266	132.105	14.702	163.032	17.487	190.995	36.772
6	2.4	86.226	4.300	129.516	7.859	169.593	19.252	205.116	33.105
7	2.8	111.192	3.024	119.403	14.953	155.418	33.261	209.415	32.677
8	3.2	82.536	9.609	119.415	1.090	174.663	21.119	192.213	55.365
9	3.6	95.427	4.595	156.141	1.863	157.125	23.911	229.119	16.026
10	4	69.708	4.464	145.395	15.866	164.598	21.173	209.745	46.806
11	4.4	63.960	4.646	156.399	7.775	165.951	23.295	207.633	43.483
12	4.8	73.947	5.489	159.819	5.719	134.970	30.135	217.296	49.395
13	5.2	95.754	3.796	150.786	1.240	170.409	30.632	205.086	34.257
14	5.6	122.325	5.582	150.387	39.127	127.182	30.632	215.520	40.413
15	6	116.196	4.177	156.093	2.604	252.342	17.487	222.810	52.488
16	6.4	118.092	10.827	160.020	5.503	140.697	19.252	211.956	43.972
17	6.8	121.809	5.493	152.649	5.112	221.715	33.261	182.780	52.213
18	7.2	123.213	10.561	126.129	14.776	184.554	21.119	245.826	68.675
19	7.6	121.953	7.271	163.254	5.779	257.130	23.911	180.000	96.815
20	8	121.956	9.373	109.570	11.097	180.114	21.173	186.570	70.913
21	8.4	125.814	6.682	150.528	20.186	170.940	23.295	245.496	73.243
22	8.8	126.042	7.424	146.403	3.362	153.258	33.261	238.257	69.578
23	9.2	123.378	6.532	159.081	28.320	152.760	21.119	231.600	118.771
24	9.6	124.068	8.498	158.157	5.631	146.346	23.911	215.145	82.765
25	10	129.522	7.520	144.060	10.789	196.293	21.173	219.399	87.207
26	10.4	123.870	6.156	155.484	19.876	195.708	23.295	270.930	71.156
27	10.8	125.691	5.998	140.706	2.308	195.438	30.135	172.470	107.978
28	11.2	114.132	3.975	162.726	12.245	201.618	30.632	260.268	95.203
29	11.6	125.646	8.733	163.254	8.618	145.386	23.295	238.407	76.663
30	12	123.438	4.636	109.570	19.419	225.867	33.261	236.577	75.309

(Cont…) Table 4.5

		Ambient (20°C)		0°C		-60°C		-120°C	
Hole No.	Machining Time (sec)	"F_z" Max (N)	"M_z" Max (N-cm)	"F_z" Max (N)	"M_z" Max (N-cm)	"F_z" Max (N)	"M_z" Max (N-cm)	"F_z" Max (N)	"M_z" Max (N-cm)
31	12.4	122.343	10.071	150.528	15.958	205.740	17.487	266.826	97.709
32	12.8	122.046	6.881	146.403	2.933	240.336	19.252	277.536	69.978
33	13.2	123.489	6.311	159.081	4.346	162.273	33.261	288.774	94.887
34	13.6	122.679	10.096	158.157	3.429	266.820	21.119	282.801	73.899
35	14	125.310	10.494	144.060	4.651	226.725	23.911	201.690	75.628
36	14.4	127.335	23.285	146.403	4.160	133.566	21.173	172.470	86.835
37	14.8	126.963	18.585	159.081	16.036	131.340	23.295	260.268	104.048
38	15.2	129.342	21.144	158.157	3.182	156.252	12.194	238.407	68.403
39	15.6	125.892	25.406	144.060	10.789	163.797	17.487	236.577	70.940
40	16	124.014	28.657	155.484	19.876	145.488	17.487	266.826	86.447
41	16.4	115.185	14.887	140.706	2.308	195.438	19.252	277.536	93.469
42	16.8	119.163	7.618	162.726	12.245	196.293	33.261	288.774	83.221
43	17.2	123.630	8.837	140.706	8.618	195.708	21.119	282.801	84.259
44	17.6	123.630	4.677	162.726	19.419	195.438	23.911	282.801	84.119
45	18	121.929	7.383	163.254	15.958	201.618	21.173	201.690	95.174
46	18.4	130.011	5.976	109.570	2.933	145.386	30.632	288.447	69.578
47	18.8	127.695	5.976	150.528	4.346	225.867	23.295	280.599	118.771
48	19.2	124.509	13.614	146.403	3.429	205.740	33.261	266.049	82.765
49	19.6	125.601	16.683	158.157	3.429	240.336	17.487	249.081	87.207
50	20	125.622	9.179	144.060	4.651	162.273	19.252	288.774	71.156
51	20.4	126.786	11.223	155.484	4.160	266.820	33.261	282.801	107.978
52	20.8	126.036	15.839	140.706	16.036	226.725	21.119	201.690	95.203
53	21.2	125.547	13.400	162.726	3.182	133.566	23.911	288.774	83.221
54	21.6	125.148	13.454	163.254	10.789	131.340	19.252	282.801	84.259
55	22	124.341	19.933	109.570	20.186	156.252	33.261	282.801	84.119
56	22.4	121.677	17.675	109.570	3.362	205.740	21.119	201.690	95.174
57	22.8	129.480	27.524	150.528	28.320	240.336	30.632	288.447	69.578
58	23.2	131.385	27.463	146.403	5.631	162.273	17.487	280.599	71.156
59	23.6	124.341	22.264	158.157	10.789	266.820	19.252	266.049	107.978
60	24	121.677	29.815	163.254	20.186	266.820	33.261	288.774	95.203

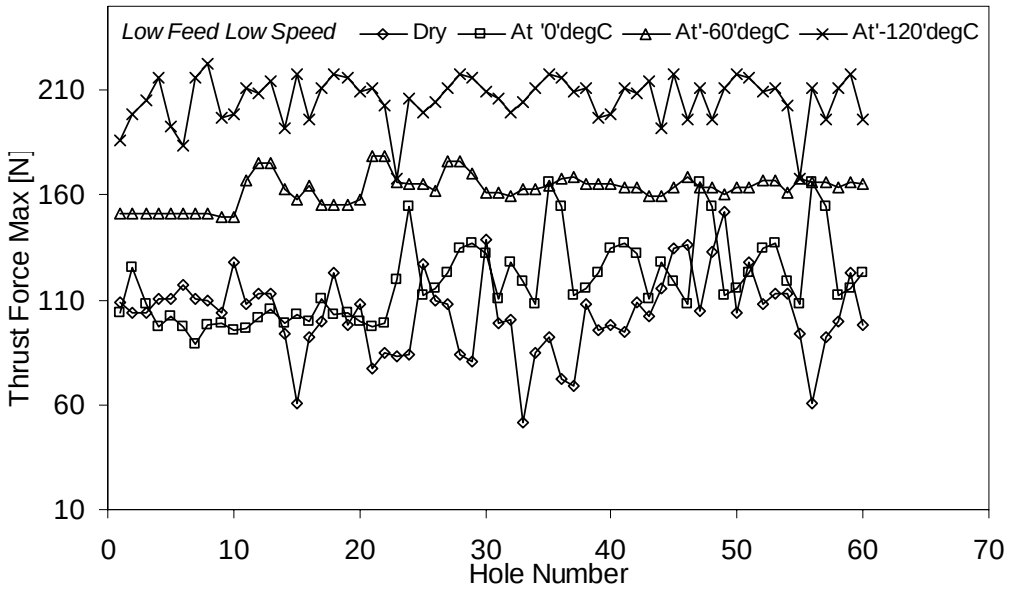

Figure 4.4: Maximum Drilling Thrust Vs No. of Holes Drilled at Low Feed Low Speed Machining Condition for Four different Workpiece Temperatures

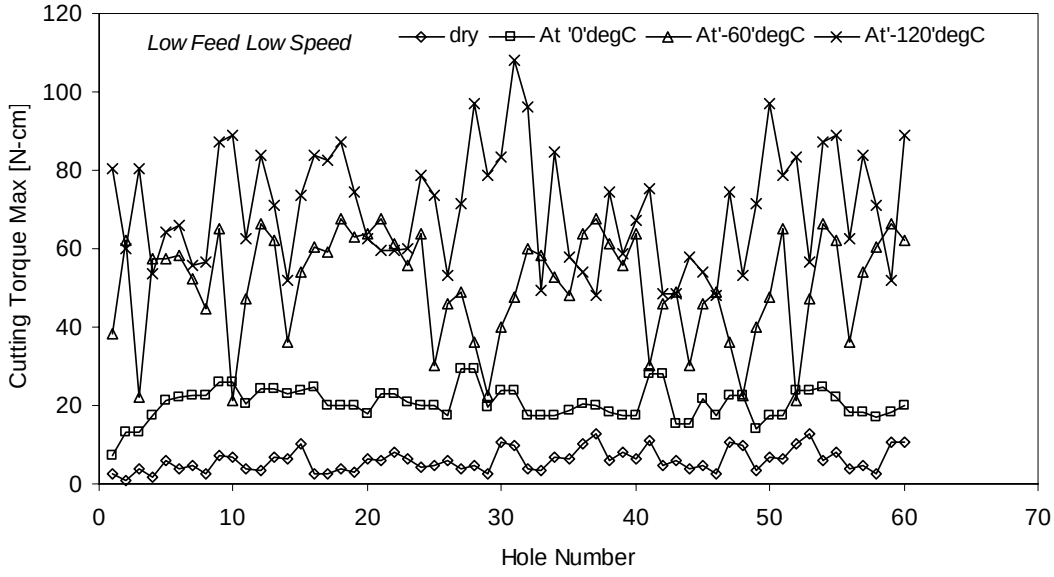

Figure 4.5: Maximum Drilling Torque Vs No. of Holes Drilled at Low Feed Low Speed Machining Condition for Four different Workpiece Temperatures

Table 4.6: Statistical Parameters of the Adequate Normal Probability Model of the Maximum Thrust Force Data of the Four Test Conditions for each of the Workpiece Temperatures

Maximum Thrust Force (N)							
Workpiece Temperature	Machining Condition	Data Points	Mean	Coef. Of Variation	Standard Deviation	Confidence Interval	
						Lower Limit	Upper Limit
20^0C (Ambient)	f_1N_1	60	102.98	0.19	19.55	98.04	107.93
	f_1N_2	60	81.07	0.37	29.73	73.55	88.59
	f_2N_1	60	192.14	0.08	16.23	188.04	196.25
	f_2N_2	60	116.86	0.14	15.78	112.86	120.85
0^0C	f_1N_1	60	118.35	0.16	19.52	113.41	123.29
	f_1N_2	60	97.54	0.06	6.31	95.94	99.13
	f_2N_1	60	169.66	0.2	33.91	161.08	178.24
	f_2N_2	60	144.78	0.12	17.86	140.26	149.30
-60^0C	f_1N_1	60	162.72	0.04	7.30	160.87	164.57
	f_1N_2	60	154.90	0.1	15.62	150.95	158.85
	f_2N_1	60	181.08	0.09	16.78	176.84	185.33
	f_2N_2	60	186.52	0.21	39.46	176.54	196.51
-120^0C	f_1N_1	60	205.63	0.06	11.36	202.76	208.50
	f_1N_2	60	179.86	0.09	15.34	175.97	183.74
	f_2N_1	60	296.34	0.12	35.69	287.32	305.37
	f_2N_2	60	240.35	0.15	36.72	231.06	249.64

Table 4.7: Statistical Parameters of the Adequate Normal Probability Model of the Maximum Torque Data of the Four Test Conditions for each of the Workpiece Temperatures

Maximum Torque (N-Cm)							
Workpiece Temperature	Machining Condition	Data Points	Mean	Coef. Of Variation	Standard Deviation	Confidence Interval	
						Lower Limit	Upper Limit
20^0C (Ambient)	f_1N_1	60	5.99	0.49	2.96	5.25	6.74
	f_1N_2	60	6.91	0.59	4.07	5.88	7.94
	f_2N_1	60	12.26	0.29	3.62	11.35	13.18
	f_2N_2	60	10.95	0.64	7.03	9.17	12.73
0^0C	f_1N_1	60	20.51	0.20	4.14	19.46	21.56
	f_1N_2	60	10.15	0.53	5.38	8.79	11.51
	f_2N_1	60	17.64	0.33	5.84	16.17	19.12
	f_2N_2	60	10.28	0.78	7.98	8.26	12.30
-60^0C	f_1N_1	60	50.80	0.27	13.70	47.33	54.26
	f_1N_2	60	16.16	0.43	6.99	14.39	17.93
	f_2N_1	60	20.65	0.42	8.67	18.46	22.84
	f_2N_2	60	23.35	0.27	6.42	21.72	24.97
-120^0C	f_1N_1	60	70.38	0.21	15.03	66.57	74.18
	f_1N_2	60	34.76	0.33	11.37	31.88	37.63
	f_2N_1	60	30.32	0.6	18.17	25.72	34.92
	f_2N_2	60	72.53	0.34	24.83	66.25	78.81

4.2.1 Effect of Workpiece Temperature on Drilling Thrust Force

The mean values of the average drilling thrust force data listed in Table 4.6 are plotted against workpiece temperature in Figure 4.6. Each data point includes an error bar that shows its degree of uncertainty relative to the respective data set obtained from the confidence intervals of the means using:

$$\text{Confidence Interval (C.I)} = \text{Mean} \pm t_{\alpha/2} \times \left(\frac{\text{Standard Deviation}}{\sqrt{\text{No. of Data Points}}} \right)$$ Where $t_{\alpha/2}$ is the Students-t-distribution evaluated at $\alpha = 0.05$.

It can be noticed from Figure 4.6 that average values of the maximum thrust force increase linearly with the decrease in workpiece temperature under all machining conditions except that with speed = 1200 rpm and feed = 0.1 mm/rev (f_2N_1). The increase in the average value of the maximum thrust force with the decrease in the workpiece temperature agrees with the fact that cooling of the fiber and resin result in an increase in their strength and stiffness. Bhattacharaya et al (11) reports that due to the difference of thermal expansion coefficients of the resin and the fiber (epoxy: 80-100x$10^{-6}/^0$K and Kevlar: about -4x$10^{-6}/^0$K and 50x$10^{-6}/^0$K in longitudinal and transverse directions, respectively) a compressive stress is induced on the fiber, which strengthens the bond between the fiber and resin. These conditions tend to increase the drilling thrust force.

When drilling the laminate at 20^0C because of the low thermal conductivity of Aramid/epoxy the heat generated during chip removal can not be dissipated and causes a concentrated heat build up in the material adjacent to the tip of the drill, thereby lowers

the mechanical strength of epoxy resin as reported by DiIlio et al [7] and results in lower drilling thrust force. The average values of the thrust force at 0^0C and -60^0C workpiece temperatures and f_2N_1 are observed to be below that of 20^0C. This sudden drop in the thrust force values seems to contradict its increasing trend with the decrease in the drilling temperature, shown by the other three machining conditions, and can thus be attributed to experimental error.

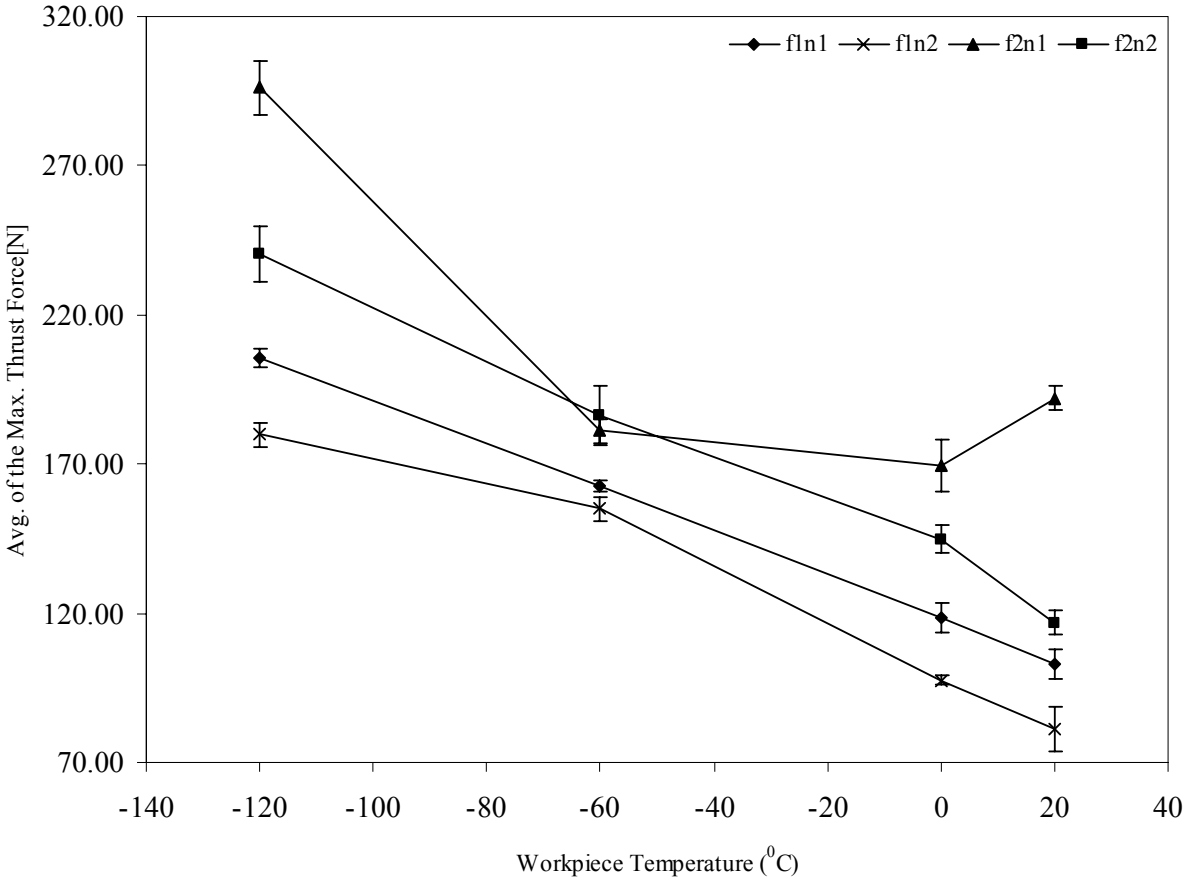

Figure 4.6: Average of Maximum Drilling Thrust Force at Various Workpiece Temperatures

The effect of speed and feed rate on the drilling thrust force can also be evaluated from the plots in Figure 4.6. The figure shows that for all levels of drilling temperature and low levels of feed rate, i.e. f=0.025 mm/rev, the effect of increasing speed from 1200 rpm to 3000 rpm is to decrease the average value of maximum thrust force. However, the difference in thrust force between the two levels of speeds at -60^0C is about half that at 20^0C, 0^0C, and -120^0C. Similar to the low level of feed, it is observed that at the high level of feed rate, i.e. f = 0.1 mm/rev, the effect of increasing the speed from 1200 to 3000 rpm is to decrease the thrust force, except for -60^0C. The decrease in thrust force with increase in speed is attributed to the fact that higher speeds generate more heat and can thus decrease the strength of the workpiece compared to the lower levels of speed. These results have been confirmed with the test of hypothesis which reveals that, at 95% confidence, the average value of the maximum thrust force at both low and high levels of feed seems to decrease with increase in cutting speed.

Figure 4.6 shows that for all levels of drilling temperature and low levels of speed, i.e. N=1200 rpm, the effect of increasing feed from 0.025 to 0.1 mm/rev is to increase the average value of maximum thrust force by about 40%. Similar to the low level of speed, it is observed that at the high level of speed, i.e. N= 3000 rpm, the effect of increasing the feed from 0.025 to 0.1 mm/rev is to increase the thrust force by 30-45%. The effect of increasing thrust force with feed rate at both levels of speed is in agreement to the findings of Won et al [48] for composite machining under ambient temperature. The possible reason mentioned was that, the thrust force contributed by the chisel edge is usually a larger fraction of the total thrust force and increases drastically with increasing

feed. Thus, the thrust component resulting from extrusion action at the chisel edge will govern the total thrust force at higher feed. Caprino et al [21] described feed rate as the critical parameter that governs the material behavior during composites drilling. He also suggested that the hole damage and the cutting forces are dependent on feed rate rather than on feed speed of spindle speed separately. It is important to note here that no data was found in the technical literature which reports on the effect of drilling parameters on thrust force at temperatures below ambient.

4.2.2 Effects of Workpiece Temperature on Drilling Torque

The mean values of the average drilling torque data listed in Table 4.7 are plotted against workpiece temperature in Figure 4.7. The figure also include the error bars of the average values of the maximum drilling torque evaluated using the formula described in the previous section.

From Figure 4.7 it is clear that that average values of the maximum torque increase with decrease in workpiece temperature under all machining conditions. This increase in torque can be explain in the manner similar to that of drilling thrust mentioned in the preceding section. Won et al [48] reported that during drilling of Aramid/epoxy laminates at ambient conditions, high machining torque generated can be attributed to increase in residual torque with increasing hole depth, which also result in fuzzy machined surface.

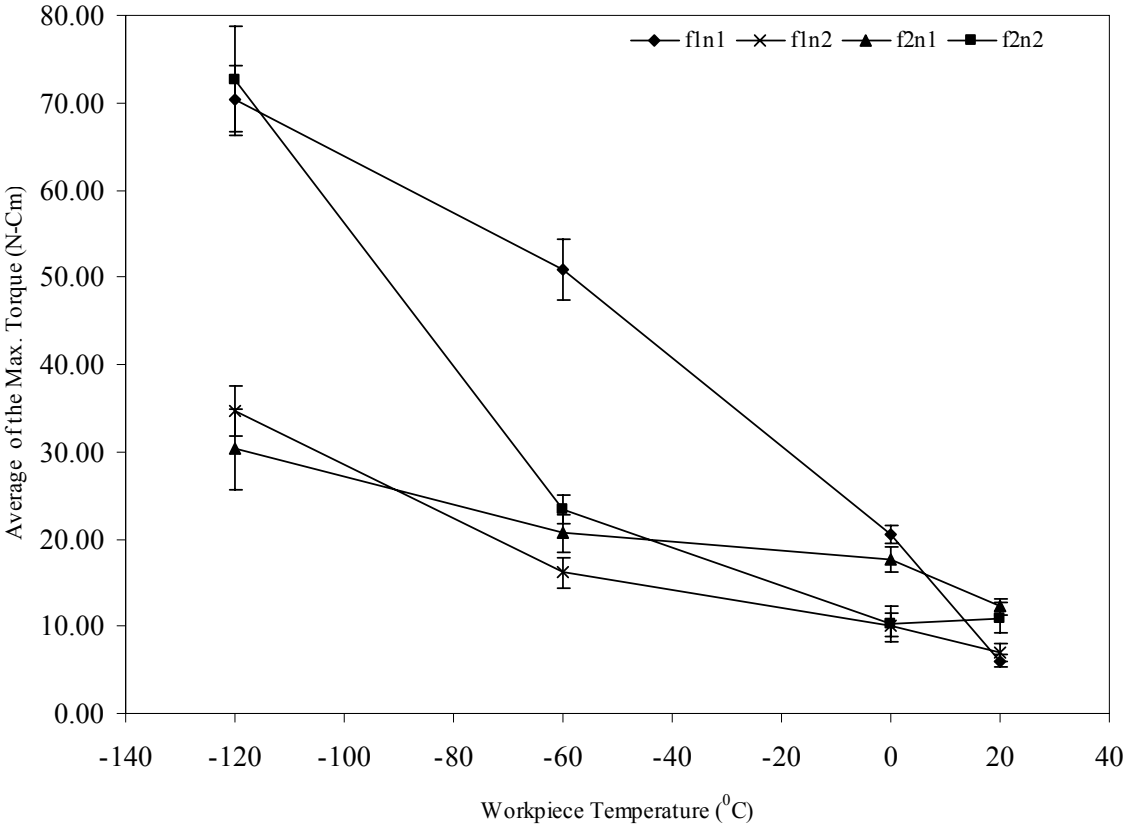

Figure 4.7: Average of Maximum Drilling Torque at Various Workpiece Temperatures

The effect of speed and feed rate on the drilling torque can also be evaluated from the plots in Figure 4.7. The figure shows that for all levels of drilling temperature and low levels of feed rate, i.e. f=0.025 mm/rev, the effect of increasing speed from 1200 rpm to 3000 rpm is to decrease the average value of maximum drilling torque, except at 20^0C where there is slight increase (about 15%)in torque with speed. However, the difference in drilling torque between the two levels of speeds at -120^0C and -60^0C is about three times that at 0^0C. Similar to the low level of feed, it is observed that at the high level of feed

rate, i.e. f = 0.1 mm/rev, the effect of increasing the speed from 1200 to 3000 rpm is to decrease the drilling torque, below -60^{0}C. The decrease in drilling torque at 0^{0}C was found to be about 25% of that at 20^{0}C. While form -60^{0}C onwards it has been noticed that the average drilling torque increased with the speed and the rate of increase was found to be maximum at -120^{0}C. These results have been confirmed with the test of hypothesis which reveals that, at 95% confidence, the average value of the maximum thrust force at both low and high levels of feed seems to decrease with increase in cutting speed.

Figure 4.7 shows that for all levels of drilling temperature and low levels of speed, i.e. N=1200, the effect of increasing feed from 0.025 to 0.1 mm/rev is to decrease the average value of maximum drilling torque for all workpiece temperatures except 20^{0}C. There was an increase of about 50% in torque value at the ambient temperature. Whereas, when the workpiece temperature was reduced below ambient the torque value has been found to decrease by about 50%. Similar to the low level of speed, it is observed that at the high level of speed, i.e. N= 3000 rpm, the effect of increasing the feed from 0.025 to 0.1 mm/rev is to increase the drilling torque by 50-55%. The effect of increasing torque with feed rate at both levels of speed is in agreement to the findings of Bhattacharaya et al (30) for Kevlar composite machining, he reported that at cryogenic temperatures the cutting force works mostly at the extreme drill radius whereas in normal situations they remain more distributed, thus reducing the effective torque arm It is important to note here that not much data was found in the technical literature reporting the effects of drilling parameters on cutting torque at temperatures below ambient.

4.2.3 Effects of Workpiece Temperature on Specific Cutting Energy

Specific cutting energy is defined as the energy consumed in removing a unit volume of material or the total energy input rate divided by material removal rate and it is a good indication of machining effort [11]. In drilling, it is calculated by

$$u = \frac{8M}{fd^2} \qquad \text{Equation 4.2}$$

Where u = specific cutting energy M = cutting torque

f = feed rate d = drill diameter

For Kevlar laminates under investigation, the specific cutting energy was calculated from the value of the average of the maximum torque value measured during machining at specified conditions using a new drill for each test condition. Table 4.8 shows the calculated values of 'u' at different test conditions of the Kevlar laminate together with their corresponding slopes of 'u' versus 'f x d' plots. The table reveals that the specific cutting energy of the Kevlar laminates is smaller for the laminates machined at ambient temperature than for that machined at cryogenic temperatures. Furthermore, the values of 'u' at the lower cutting speed (1200 rpm) are higher than those of the higher cutting speed (3000 rpm). This is attributed to the softening effect of the heat generated at high cutting speeds. Figure 4.8 shows the specific cutting energy 'u' obtained from Equation (4.2) for measured values of cutting torque (M) plotted against (fxd) on log-log coordinates.

It is reported by Hocheng et al [12] that milder the slope, less cutting effort is required. On the other hand, if the slope is steeper the cutting energy is larger. The slopes

of 'u' verses 'fxd' are in the range of – 0.127 to - 0.510 when drilling was performed at 1200 rpm and in the range of – 0.1 to – 0.27 when drilling was done at 3000 rpm. Furthermore, the slopes for the laminates drilled at cryogenic temperatures are significantly steeper than for dry machined ones. The values of slope obtained here are in agreement with the findings of Shuaib et al [55] calculated the slope of – 0.5 for KFRP at dry conditions. The slopes for some material as reported in literature were – 0.19 for Glass-Peek [12], - 0.2 for Glass-E [12] and – 0.34 for Carbon/Epoxy. From the values of specific cutting energy it is clear that at -120^0C is the optimum work piece temperature at higher machining speed the energy consumed is low when compared to those at other temperature levels. But for lower machining speed the energy consumed is less at ambient temperature. Therefore it can be concluded that for machining economy with respect to energy the optimum machining temperature will be at -120^0C (high speeds)for the composite that are under test.

The effect of workpiece temperature and drilling parameters on the specific cutting energy are evaluate using the estimated statistical parameters (mean and standard deviation) of the adequate normal probability models listed in Table 4.9. Variations of specific cutting energy with workpiece temperature are shown plotted in Figure 4.9. It is clear from the plots that decrease in workpiece temperature will increase the specific cutting energy which is quite possible as it varies proportionately with drilling torque and any increase in torque value will increase the specific cutting energy. The specific cutting energy for low 'fxd' value (0.15) seems to be higher for low cutting speeds and a significant difference has been noticed in the specific cutting energy when the workpiece

temperature was reduced. The value of specific cutting energy for high 'fxd'= 0.6 seems independent of cutting speed till -60^{0}C as the values for both speed is almost close to each other. But there has been a significant increase when the workpiece temperature was reduced to -120^{0}C. It is clear that the specific energy decreases with increase in 'fxd' value as it is inversely related to the feed rate.

Table 4.8: Specific Cutting Energy u and the Slope of the Curve of u vs. fxd

Specimen Temperature	Drilling Speed N=1200 rpm		Slope	Drilling Speed N=3000 rpm		Slope
	Specific Cutting Energy (MJ/m^3)			Specific Cutting Energy (MJ/m^3)		
	f x d = 0.15	f x d = 0.6		f x d = 0.15	f x d = 0.6	
20^0C	532.81	272.52	-0.127	614.27	243.27	-0.200
0^0C	1823.08	392.10	-0.330	902.34	228.47	-0.270
-60^0C	4515.21	458.86	-0.510	1436.31	518.83	-0.210
-120^0C	6255.74	673.76	-0.490	3089.39	1611.81	-0.140

Table 4.9: Statistical Parameters of the Adequate Normal Probability Models of the Specific Cutting Energy Data of the Four Test Conditions for Each of the Workpiece Temperatures

Specific Cutting Energy (MJ/m^3)							
Workpiece Temperature	Machining Condition	Data Points	Mean	Coef. of Variation	Standard Deviation	Confidence Interval	
						Lower Limit	Upper Limit
20^0C (Ambient)	f_1N_1	60	532.81	0.49	263.04	466.25	599.37
	f_1N_2	60	1823.08	0.20	367.62	1730.06	1916.10
	f_2N_1	60	4515.21	0.27	1217.57	4207.13	4823.29
	f_2N_2	60	6255.74	0.21	1336.15	5917.66	6593.83
0^0C	f_1N_1	60	614.27	0.59	362.14	522.64	705.90
	f_1N_2	60	902.34	0.53	478.38	781.30	1023.39
	f_2N_1	60	1436.31	0.43	621.72	1279.00	1593.62
	f_2N_2	60	3089.39	0.33	1010.81	2833.62	3345.15
-60^0C	f_1N_1	60	272.52	0.29	80.35	252.19	292.86
	f_1N_2	60	392.10	0.33	129.68	359.29	424.92
	f_2N_1	60	458.86	0.42	192.59	410.13	507.59
	f_2N_2	60	673.76	0.60	403.81	571.58	775.94
-120^0C	f_1N_1	60	243.27	0.64	156.32	203.72	282.83
	f_1N_2	60	228.47	0.78	177.33	183.60	273.34
	f_2N_1	60	518.83	0.27	142.65	482.74	554.93
	f_2N_2	60	1611.81	0.34	551.85	1472.17	1751.44

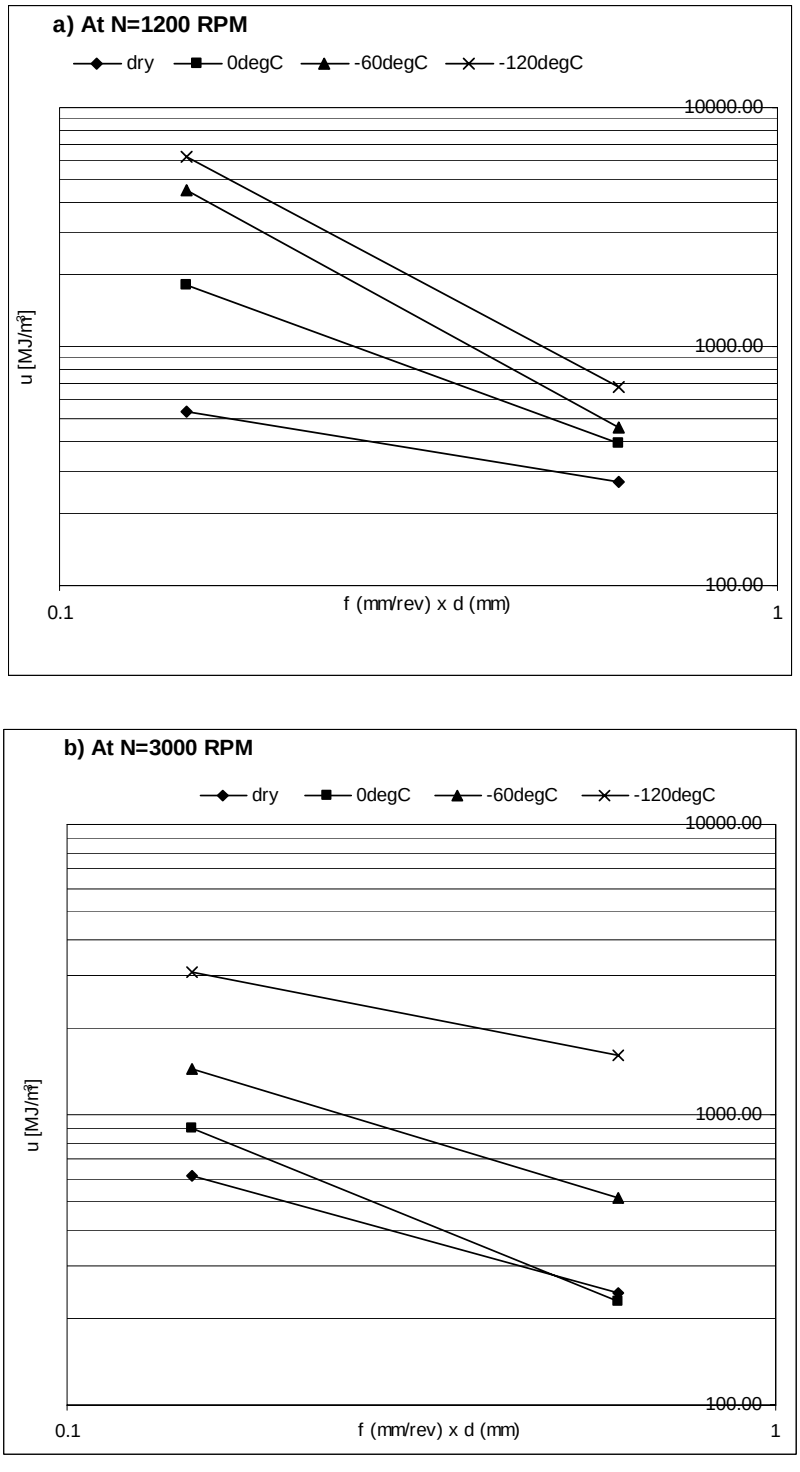

Figure 4.8: Specific Cutting Energy as a Function of 'fxd' for different Machining Speed

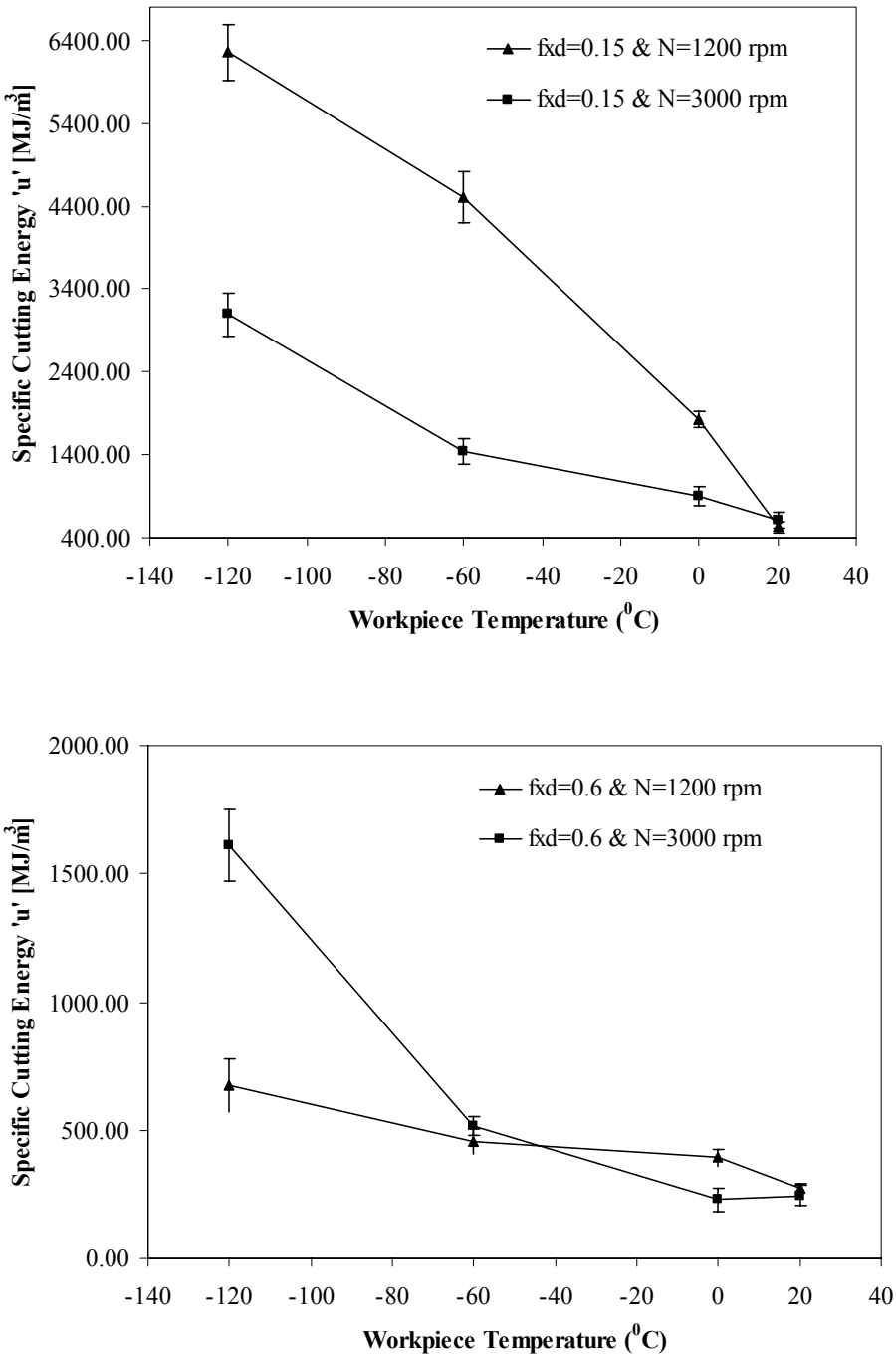

Figure 4.9: Specific Cutting Energy as a Function of Workpiece Temperature for different' fxd' and Machining Speed Combination

CHAPTER 5

RESULTS AND DISCUSSION OF HOLE QUALITY

This chapter describes the evaluation of the effect of workpiece temperature and machining parameters on the quality of the holes that are drilled using TiN coated HSS drills through the Kevlar composite laminates. The criteria for assessing the hole quality in composite materials includes the width of the delaminated region around the hole periphery, the hole dimensions, and length and density of remnant fibers at the entry and exit sides of the hole. Shuaib et al [51] reported that during drilling the Kevlar composite laminates at room temperature extensive damage in terms of delamination and disbonding can occur and appear as narrow ring zone around the periphery of the entry and exit sides of the hole. The quality of the hole is dependent on the width of this zone in addition to several other factors.

A term called 'delamination factor' [28] will be used to asses the extent of the delamination damage and evaluate the effect of the drilling temperature of the composite laminates and machining conditions on the quality of drilled holes. The delamination factor, 'F_d', is the ratio of the maximum area of the damaged zone to the cross sectional area of the hole: $F_d = \frac{A_d}{A_i}$ Equation 5.1

Where $A_d = \frac{\pi}{4} * (d_0{}^2 - d_i{}^2)$ and $A_i = \frac{\pi}{4} * (d_i{}^2)$ also 'd_o' is the outer diameter of delamination zone and 'd_i' is the diameter of the drilled hole. These diameters are measured from optical images of the holes that are drilled through the Kevlar composite laminates.

The delamination factor, 'F_d' is calculated for each hole and listed in Table 5.1 through Table 5.4 for the different cutting conditions and workpiece drilling temperatures. The plots of 'F_d' against the number of holes drilled shown in Figure 5.1 indicate that for drilling at room temperature, 20^0C, the value of the delamination factor fluctuates around a value of about 1.2 until the 40^{th} hole, and then starts an increasing trend to about 1.8 at the 60^{th} hole. On the other hand, for the other three workpiece temperatures (0^0C, -60^0C, -120^0C) 'F_d' values appear to fluctuate around 0.3-0.4 from the first to the last drilled hole. This indicates an improvement of about 400% in the delamination damage when drilling is performed at lower temperature compared with that at room temperature. Similar to the drilling forces, the variation of 'F_d' with the number of holes drilled at a certain workpiece temperature was found to be represented by a normal distribution. The statistical parameters (i.e. mean, standard deviation, coefficient of variation) of the models corresponding to the 'F_d' data sets are listed in Table 5.5. The table also includes the 95% confidence intervals of the respective means of the data sets.

Table 5.1: Delamination Ratio of Kevlar Laminates at 20^0C (Ambient) Workpiece Temperature

Hole No.	f_1N_1	f_1N_2	f_2N_1	f_2N_2	Hole No.	f_1N_1	f_1N_2	f_2N_1	f_2N_2
1	1.289	0.844	1.15	0.96	31	1.218	0.905	1.258	0.721
2	1.252	0.854	0.949	0.612	32	1.284	0.889	0.919	0.799
3	1.221	0.856	0.970	0.679	33	1.261	0.924	0.941	0.725
4	1.272	0.904	1.070	0.727	34	1.259	0.865	1.019	0.722
6	1.214	0.908	0.977	0.717	36	1.302	0.940	1.089	0.723
9	1.265	0.884	0.949	0.727	39	1.319	0.978	0.992	0.737
10	1.191	0.870	1.136	0.732	40	1.326	0.901	1.084	0.729
11	1.177	0.909	1.131	0.721	41	1.325	0.872	1.041	0.643
12	1.191	0.915	1.127	0.804	42	1.375	0.872	1.260	0.726
13	1.183	0.874	0.929	0.804	43	1.413	0.978	1.330	0.722
14	1.005	0.854	0.921	0.773	44	1.378	0.805	1.383	0.706
15	1.106	0.862	1.219	0.726	45	1.385	0.965	1.287	0.742
16	1.292	0.889	1.232	0.733	46	1.395	1.046	1.320	0.769
17	1.170	0.882	1.240	0.731	47	1.405	1.250	1.185	0.758
18	1.196	0.881	1.122	0.737	48	1.396	1.111	1.166	0.933
19	1.196	0.905	0.870	0.712	49	1.377	1.381	1.117	0.955
20	1.195	0.889	0.889	0.719	50	1.402	1.217	1.100	0.823
21	1.036	0.924	1.005	0.781	51	1.417	1.337	1.116	0.815
22	1.114	0.865	1.202	0.758	52	1.424	1.244	1.201	0.911
23	1.137	0.940	1.129	0.742	53	1.408	1.215	1.258	0.768
24	1.109	1.097	1.199	0.742	54	1.341	1.343	1.261	0.965
25	1.063	0.971	1.106	0.735	55	1.376	1.432	1.255	0.927
26	1.144	0.957	1.012	0.727	56	1.401	1.449	1.263	0.906
27	1.183	0.845	0.933	0.691	57	1.411	1.436	1.392	0.833
28	1.034	0.821	1.041	0.727	58	1.569	1.417	1.408	0.841
29	1.201	0.883	1.115	0.682	59	1.618	1.481	1.480	0.889
30	1.151	1.068	0.882	0.723	60	1.79	1.431	1.395	1.25

Table 5.2: Delamination Ratio of Kevlar Laminates at 0^0C Workpiece Temperature

Hole No.	f_1N_1	f_1N_2	f_2N_1	f_2N_2	Hole No.	f_1N_1	f_1N_2	f_2N_1	f_2N_2
1	0.300	0.164	0.218	0.353	31	0.356	0.247	0.284	0.364
2	0.230	0.205	0.222	0.369	32	0.362	0.287	0.295	0.334
3	0.379	0.119	0.289	0.361	33	0.377	0.268	0.276	0.396
4	0.366	0.235	0.288	0.347	34	0.382	0.296	0.243	0.399
6	0.343	0.282	0.265	0.342	36	0.381	0.280	0.282	0.381
9	0.290	0.260	0.243	0.353	39	0.363	0.285	0.290	0.321
10	0.342	0.242	0.277	0.369	40	0.426	0.277	0.266	0.342
11	0.357	0.239	0.260	0.379	41	0.440	0.334	0.266	0.333
12	0.353	0.252	0.243	0.359	42	0.454	0.341	0.256	0.295
13	0.365	0.255	0.267	0.354	43	0.435	0.345	0.341	0.334
14	0.252	0.256	0.230	0.351	44	0.439	0.356	0.375	0.351
15	0.381	0.250	0.235	0.386	45	0.449	0.357	0.356	0.392
16	0.406	0.244	0.231	0.333	46	0.475	0.351	0.349	0.412
17	0.351	0.243	0.277	0.294	47	0.391	0.432	0.321	0.333
18	0.363	0.286	0.252	0.339	48	0.381	0.422	0.345	0.417
19	0.273	0.243	0.256	0.375	49	0.375	0.328	0.385	0.375
20	0.403	0.235	0.258	0.307	50	0.375	0.342	0.351	0.417
21	0.358	0.287	0.256	0.342	51	0.363	0.356	0.343	0.386
22	0.396	0.256	0.264	0.360	52	0.378	0.360	0.328	0.426
23	0.337	0.253	0.205	0.393	53	0.356	0.430	0.360	0.432
24	0.260	0.243	0.264	0.324	54	0.379	0.515	0.360	0.449
25	0.303	0.321	0.273	0.408	55	0.362	0.489	0.390	0.456
26	0.354	0.241	0.205	0.386	56	0.386	0.477	0.362	0.458
27	0.370	0.287	0.251	0.331	57	0.425	0.334	0.379	0.433
28	0.243	0.298	0.284	0.373	58	0.479	0.412	0.365	0.457
29	0.381	0.246	0.299	0.366	59	0.608	0.452	0.377	0.459
30	0.382	0.295	0.280	0.347	60	0.610	0.563	0.370	0.386

Table 5.3: Delamination Ratio of Kevlar Laminates at -60^{0}C Workpiece Temperature

Hole No.	f_1N_1	f_1N_2	f_2N_1	f_2N_2	Hole No.	f_1N_1	f_1N_2	f_2N_1	f_2N_2
1	0.442	0.344	0.243	0.138	31	0.421	0.375	0.202	0.145
2	0.495	0.226	0.216	0.110	32	0.466	0.321	0.148	0.141
3	0.444	0.264	0.272	0.127	33	0.493	0.360	0.197	0.131
4	0.439	0.252	0.187	0.131	34	0.422	0.299	0.182	0.124
6	0.467	0.275	0.172	0.120	36	0.421	0.247	0.179	0.170
9	0.448	0.288	0.166	0.117	39	0.499	0.375	0.194	0.131
10	0.404	0.299	0.169	0.134	40	0.484	0.339	0.170	0.130
11	0.484	0.235	0.159	0.120	41	0.467	0.205	0.223	0.134
12	0.395	0.389	0.176	0.131	42	0.471	0.282	0.184	0.138
13	0.395	0.256	0.156	0.124	43	0.492	0.342	0.141	0.134
14	0.313	0.348	0.212	0.126	44	0.473	0.256	0.138	0.141
15	0.305	0.265	0.180	0.127	45	0.468	0.288	0.268	0.127
16	0.318	0.256	0.166	0.120	46	0.457	0.277	0.212	0.148
17	0.339	0.273	0.148	0.117	47	0.457	0.222	0.289	0.145
18	0.365	0.252	0.268	0.113	48	0.467	0.320	0.330	0.134
19	0.389	0.226	0.235	0.134	49	0.465	0.243	0.326	0.134
20	0.467	0.226	0.210	0.138	50	0.512	0.344	0.244	0.158
21	0.356	0.264	0.214	0.138	51	0.542	0.226	0.184	0.148
22	0.360	0.252	0.243	0.127	52	0.543	0.264	0.141	0.145
23	0.332	0.257	0.202	0.131	53	0.523	0.252	0.223	0.173
24	0.321	0.299	0.191	0.123	54	0.526	0.275	0.240	0.120
25	0.316	0.172	0.223	0.134	55	0.541	0.452	0.148	0.127
26	0.422	0.194	0.195	0.145	56	0.562	0.300	0.173	0.141
27	0.349	0.265	0.163	0.152	57	0.532	0.408	0.134	0.208
28	0.366	0.193	0.251	0.156	58	0.567	0.344	0.285	0.204
29	0.422	0.286	0.260	0.142	59	0.516	0.304	0.343	0.208
30	0.437	0.256	0.202	0.148	60	0.584	0.488	0.252	0.310

Table 5.4 Delamination Ratio of Kevlar Laminates at -120^{0}C Workpiece Temperature

Hole No.	f_1N_1	f_1N_2	f_2N_1	f_2N_2	Hole No.	f_1N_1	f_1N_2	f_2N_1	f_2N_2
1	0.336	0.218	0.066	0.056	31	0.278	0.168	0.056	0.024
2	0.265	0.205	0.110	0.041	32	0.256	0.197	0.122	0.020
3	0.265	0.269	0.106	0.034	33	0.264	0.172	0.034	0.034
4	0.280	0.221	0.056	0.040	34	0.321	0.172	0.070	0.024
6	0.226	0.310	0.122	0.031	36	0.342	0.201	0.120	0.031
9	0.286	0.285	0.034	0.034	39	0.308	0.216	0.145	0.048
10	0.265	0.239	0.070	0.031	40	0.334	0.219	0.159	0.070
11	0.251	0.190	0.066	0.040	41	0.396	0.223	0.112	0.052
12	0.272	0.243	0.110	0.056	42	0.381	0.247	0.174	0.048
13	0.218	0.193	0.106	0.089	43	0.375	0.230	0.063	0.022
14	0.296	0.201	0.045	0.031	44	0.364	0.269	0.056	0.038
15	0.222	0.168	0.066	0.027	45	0.375	0.254	0.048	0.059
16	0.235	0.185	0.074	0.024	46	0.406	0.243	0.104	0.041
17	0.256	0.239	0.051	0.031	47	0.356	0.273	0.164	0.034
18	0.269	0.231	0.044	0.089	48	0.381	0.205	0.068	0.040
19	0.209	0.243	0.053	0.093	49	0.356	0.239	0.069	0.013
20	0.248	0.209	0.091	0.041	50	0.339	0.209	0.052	0.038
21	0.269	0.229	0.048	0.027	51	0.326	0.205	0.048	0.069
22	0.260	0.260	0.078	0.027	52	0.432	0.277	0.048	0.038
23	0.316	0.209	0.059	0.038	53	0.358	0.197	0.104	0.105
24	0.289	0.269	0.080	0.041	54	0.378	0.247	0.169	0.104
25	0.281	0.205	0.088	0.013	55	0.367	0.256	0.091	0.101
26	0.248	0.247	0.073	0.013	56	0.322	0.351	0.137	0.152
27	0.216	0.264	0.095	0.020	57	0.382	0.273	0.137	0.140
28	0.226	0.205	0.086	0.038	58	0.309	0.391	0.151	0.137
29	0.281	0.180	0.051	0.070	59	0.356	0.325	0.178	0.147
30	0.256	0.286	0.045	0.067	60	0.399	0.351	0.191	0.152

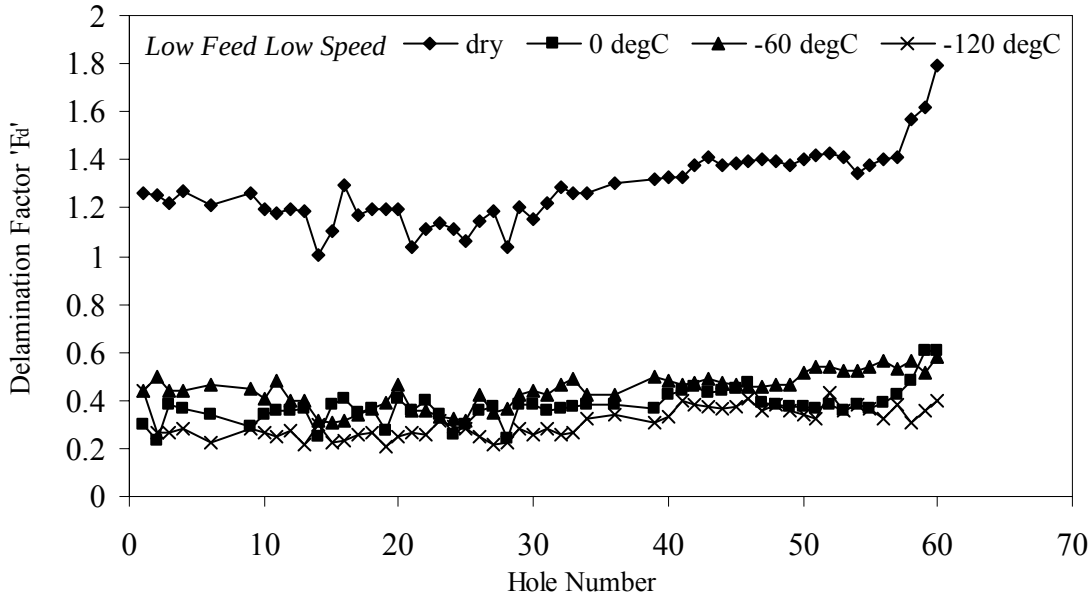

Figure 5.1: Delamination Factor 'F_d' Vs Hole No. at Low Feed Low Speed Machining Conditions for Four different Workpiece Temperatures

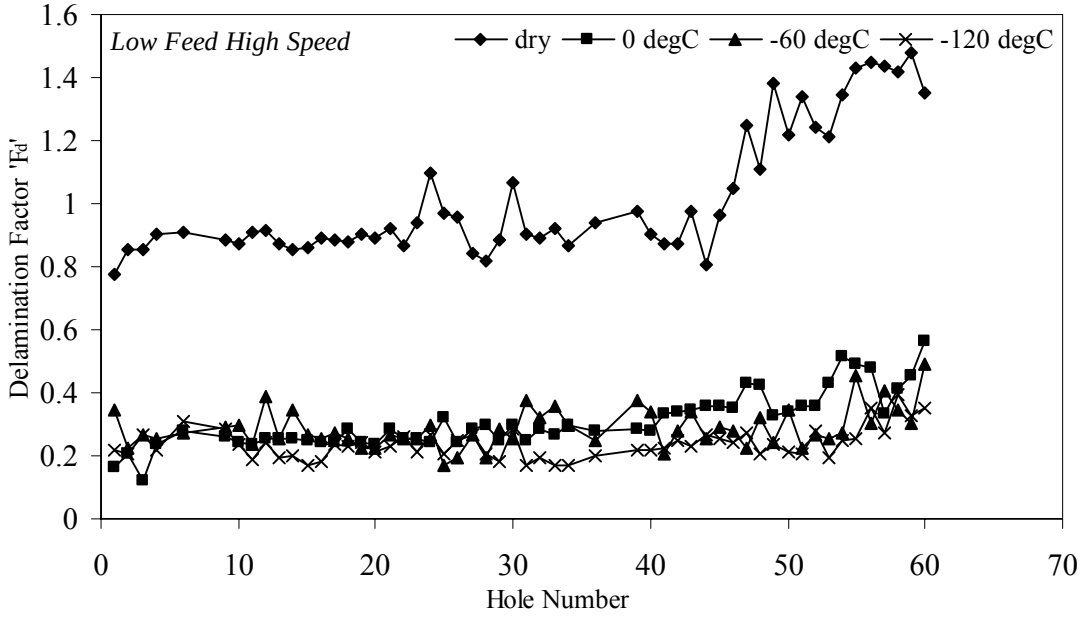

Figure 5.2: Delamination Factor 'F_d' Vs Hole No. at Low Feed High Speed Machining Conditions for Four different Workpiece Temperatures

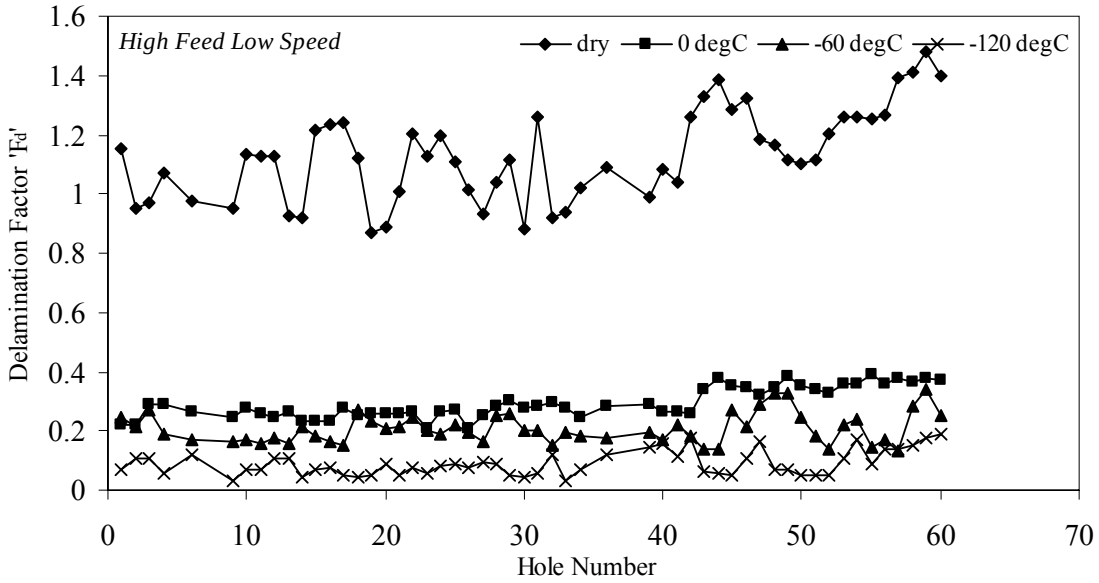

Figure 5.3: Delamination Factor 'F_d' Vs Hole No. at High Feed Low Speed Machining Conditions for Four different Workpiece Temperatures

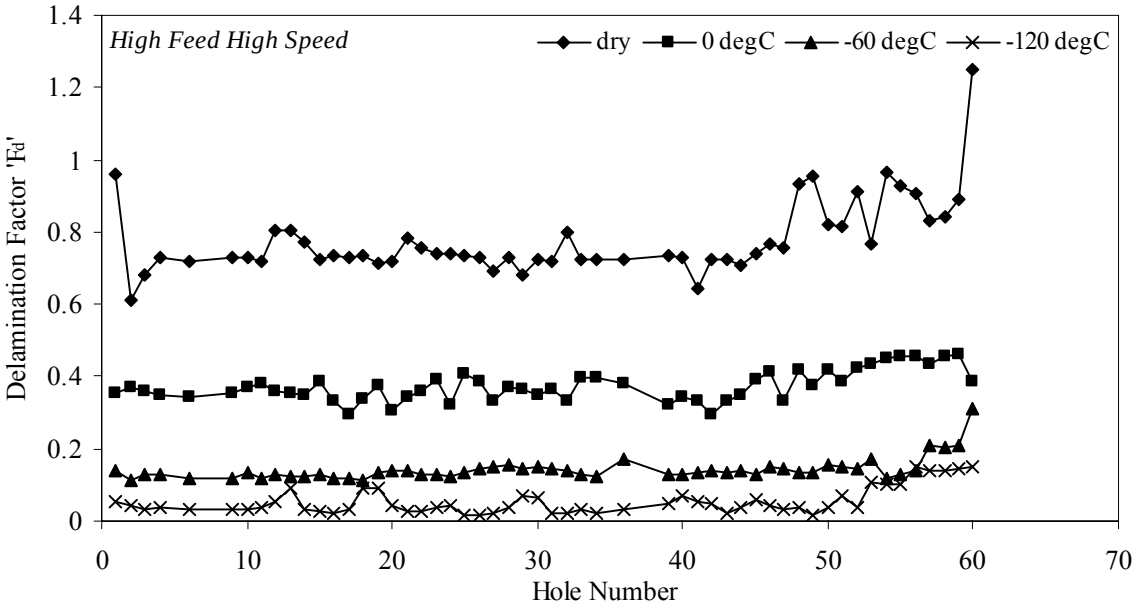

Figure 5.4: Delamination Factor 'F_d' Vs Hole No. at High Feed High Speed Machining Conditions for Four different Workpiece Temperatures

Table 5.5: Statistical Parameters of the Delamination Factor Data for the Kevlar Laminates at given Drilling Conditions.

Delamination Factor 'F_d'						
Workpiece Temperature	Machining Condition	No of Data Points	Mean	Standard Deviation	Confidence Interval	
					Lower Limit	Upper Limit
20^0C (Ambient)	f_1N_1	60	1.28	0.15	1.24	1.32
	f_1N_2	60	1.02	0.20	0.96	1.07
	f_2N_1	60	1.13	0.15	1.09	1.17
	f_2N_2	60	0.78	0.10	0.75	0.80
0^0C	f_1N_1	60	0.38	0.07	0.36	0.39
	f_1N_2	60	0.31	0.09	0.29	0.33
	f_2N_1	60	0.29	0.05	0.28	0.31
	f_2N_2	60	0.37	0.04	0.36	0.38
-60^0C	f_1N_1	60	0.44	0.07	0.43	0.46
	f_1N_2	60	0.29	0.06	0.27	0.30
	f_2N_1	60	0.21	0.05	0.20	0.22
	f_2N_2	60	0.14	0.03	0.13	0.15
-120^0C	f_1N_1	60	0.31	0.06	0.29	0.32
	f_1N_2	60	0.24	0.05	0.23	0.25
	f_2N_1	60	0.09	0.04	0.08	0.10
	f_2N_2	60	0.05	0.04	0.04	0.06

5.1 Effect of Workpiece Temperature on Hole Quality

The mean values of the average delamination factor 'F_d' data listed in Table 5.5 are plotted against workpiece temperature in Figure 5.5. Each data point includes an error bar that shows its degree of uncertainty relative to the respective data set obtained from the confidence intervals of the means using the formula described in section 4.2.

It can be noticed from Figure 5.5 that the average delamination factor 'F_d' decreases with the decrease in workpiece temperature under all machining conditions. This reduction is high at the initial drop of the workpiece temperature from ambient to 0^0C. Whereas from 0^0C to -60^0C the reduction seems to be less at low feed rates and from -60^0C to -120^0C there is a noticeable reduction in 'F_d'. This reduction in 'F_d' value at lower workpiece temperature compared to dry condition, can be explained with the help of the fact that at dry conditions, increase in temperature during drilling due to rubbing of the chip material causes matrix smearing and fiber burn.. Also at low temperature the test piece laminate material has a changed behavior due to the difference of thermal expansion coefficients of the resin and the fibre. This changed behavior induces a compressive stress on the fibre, producing a clamping force and causing the epoxy to become stiffer at cryogenic temperature resulting in fibres being held in more rigid fashion. This would in turn help in changing the failure mode from one of the bending induced rupture to that of shear fracture producing a cleaner hole Bhattacharaya et al (30). Won et al [48] reported that higher residual torques causes extensive pulled out and crushed fibre bundles that tend to clog the hole as drilling progresses, the characteristic behavior of the fibres of

Aramid/epoxy laminates to form fibrils while being cut results in high local flexibility and toughness.

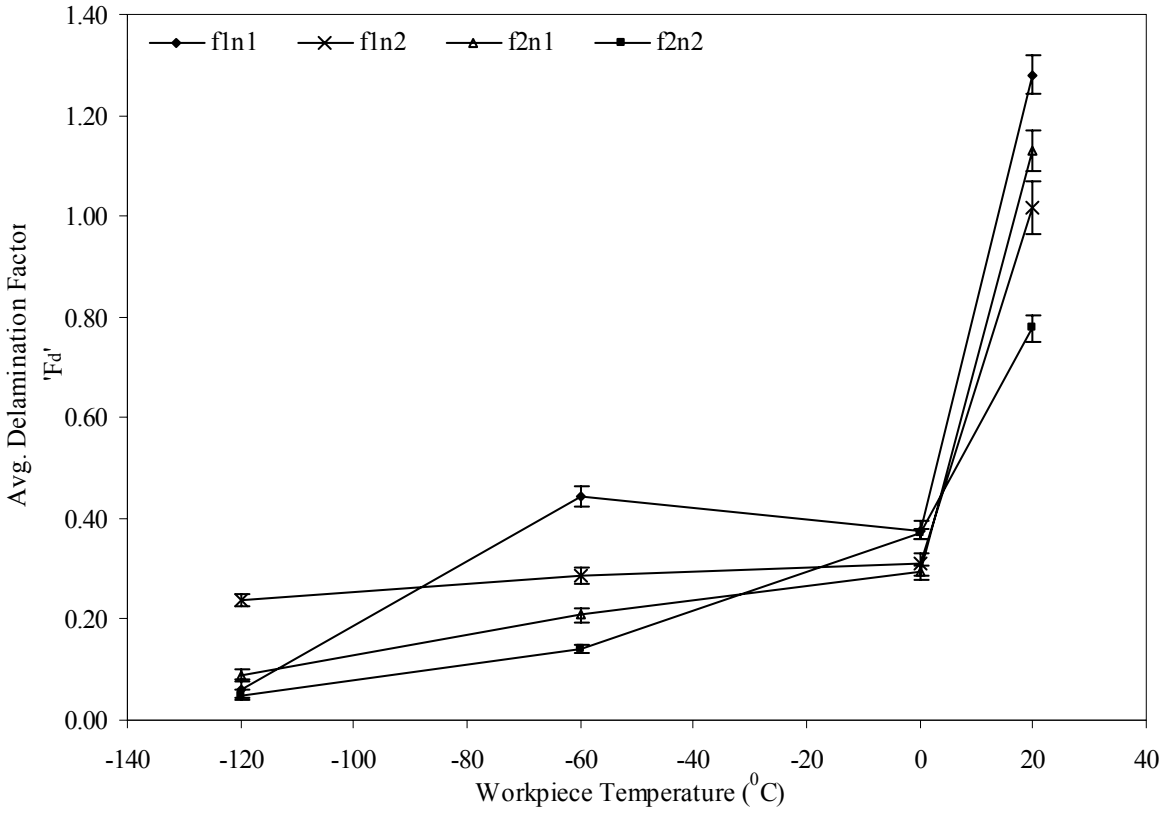

Figure 5.5: Average Delamination Factor 'F_d' at Various Workpiece Temperatures

The effect of speed and feed rate on the delamination factor 'F_d' can also be evaluated from the plots in Figure 5.5. The figure shows that for all levels of drilling temperature and low levels of feed rate, i.e. f=0.025 mm/rev, the effect of increasing speed from 1200 rpm to 3000 rpm is to decrease the average value of delamination factor 'F_d'. However, the difference in 'F_d' between the two levels of speeds at 20^0C is twice that at 0^0C, -60^0C, and

-120^{0}C. Similar to the low level of feed, it is observed that at the high level of feed rate, i.e. f = 0.1 mm/rev, the effect of increasing the speed from 1200 to 3000 rpm is to decrease the delamination factor 'F_d', except for 0^{0}C. Di Ilio et al [7] reported the additional problem that usually arises when Aramid/ epoxy laminates are machined, owing to the high toughness and low compressive resistance of the fibres which buckles under bending stresses instead of getting sheared off. This results in rough and fuzzy cut surfaces with low dimensional precision but high cutting speeds and low cutting feed greatly improves the quality of holes at ambient temperatures. It is also clear that the decrease in delamination factor at low feed rate is less (about 20%) compared to reduction at high feed rate (about 32%) when increasing speed from 1200 to 3000 rpm. This is in agreement with Hocheng et al [12] who reported that machining composites having thermoset resin (epoxy) at ambient temperature shows visible chipping at high cutting speed combined with low feed rate causing the edge of the hole to get affected greatly. High cutting speed generates large amount of heat accompanied with slow tool progression at low feed rates. Due to low thermal conductivity and transition temperature of the plastics, the accumulated heat stagnate around the tool edge destroying the matrix stability behind the tool edge and produces fuzzy and rough cuts during machining. These results have been confirmed with the test of hypothesis which reveals that, at 95% confidence, the average value of the delamination factor (F_d), at both low and high levels of feed seems to decrease with increase in cutting speed.

Figure 5.5 shows that for all levels of drilling temperature and low levels of speed, i.e. N=1200 rpm, the effect of increasing feed from 0.025 to 0.1 mm/rev is to decrease the

average value of delamination factor 'F_d' by 10-70%. Similar to the low level of speed, it is observed that at the high level of speed, i.e. N= 3000 rpm, the effect of increasing the feed from 0.025 to 0.1 mm/rev is to decrease delamination factor 'F_d' by 15-80%. The reason for reduction in 'F_d' can be due to the workpiece laminates getting chilled more at low temperatures, turning it into near brittle material. At this stage when the drill stars piercing it shears the fibre material rather than bending and tearing that happens at ambient temperature. The fibre ends of the material drilled at low temperature gets along hole wall indicating shearing whereas at ambient temperature the fibres are crushed and are smeared across the hole walls, these results seem to agree with Bhatacharaya et al [30]. But Wen et al [28] reported that at low feed rate it is likely that there is reduction in delamination, but if feed rate is too low the cutting time at the same place will be long, which increases the chances of delamination owing to deviation effects by vibration in the high spindle speed. These results have been confirmed with the test of hypothesis which reveals that, at 95% confidence, the average value of the delamination factor 'F_d', at both low and high levels of speed seems to decrease with increase in feed.

The effect of feed on average value of delamination factor 'F_d' was also evaluated using the test of hypothesis with 95% confidence level. It was noticed that for all workpiece temperatures except 0^0C and speed levels (low or high) the 'F_d' value seems to increase with increase in feed rate. For the holes drilled at 0^0C workpiece temperature the average of 'F_d' value at low speed seems to increase with increase in feed rate, while at high speed it decreases with increase in feed. Di Ilio et al [7] reported about the additional problem that usually arises when Aramid/ epoxy laminates are machined, owing to the

high toughness and low compressive resistance of the fibres which buckles under bending stresses instead of getting sheared off. This results in rough and fuzzy cut surfaces with low dimensional precision. High cutting speeds and low cutting feed can greatly improves the quality of holes at ambient temperatures. Figure 5.6 shows images of the first and the last drilled holes at dry and low work piece temperature for different machining conditions.

First hole Last hole

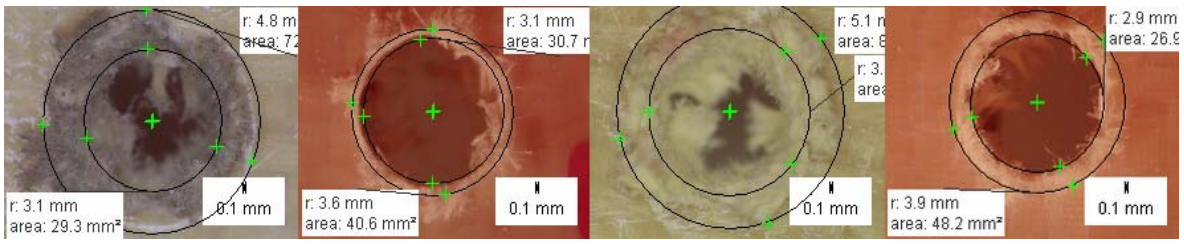

I) At f_1N_1

First hole Last hole

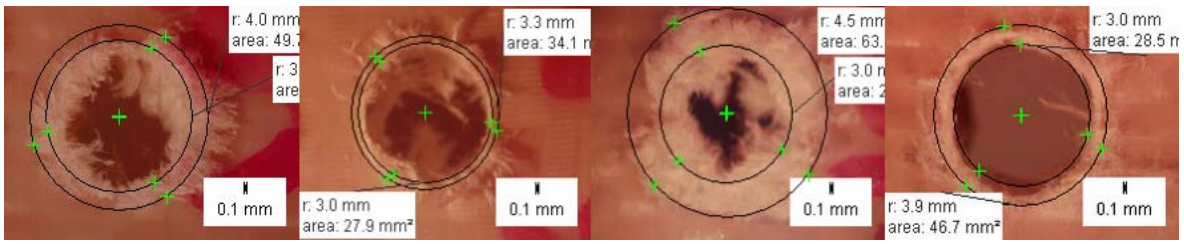

II) At f_1N_2

First hole Last hole

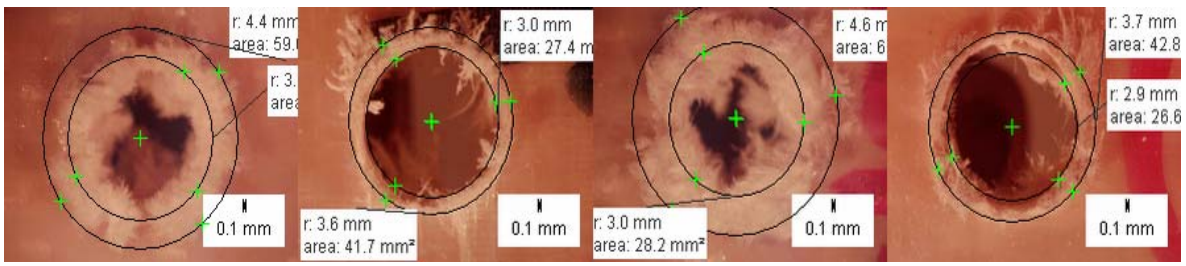

III) At f_2N_1

First hole Last hole

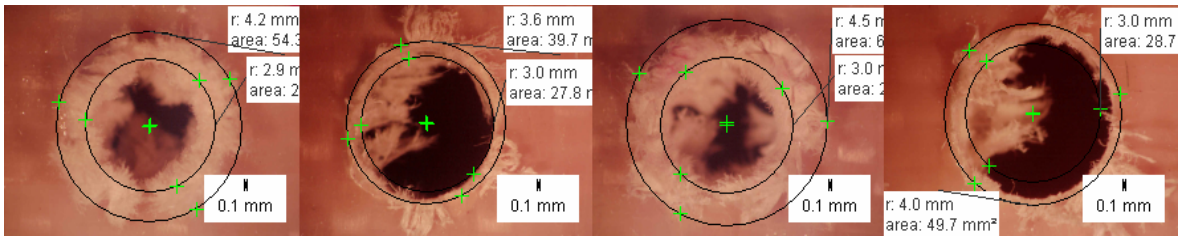

IV) At f_2N_2

Figure 5.6: Optical Photographs of First and Last Hole of Kevlar^{TM} Laminate Drilled at Ambient and -120^{0}C Workpiece Temperatures

CHAPTER 6

CONCLUSIONS AND RECOMMENDATIONS

The machinability of Kevlar^{TM} fibre reinforced composite laminates drilled using 135^0 split point TiN coated 6 mm diameter HSS drills have been investigated in this research. The effect of lowering the workpiece temperature on the machinability of the Kevlar^{TM} composite laminates are assessed using drilling thrust force, cutting torque, specific cutting energy and hole quality.

The detailed conclusions derived from this investigation and experimental results are as follows.

- With increase in number of holes drilled, thrust force and torque data was found to fluctuate around a certain value for each test condition and does not show a clear trend with machining time. Normal probability distribution has been found to be the adequate distribution model to represent this behavior for all data sets of Kevlar^{TM} composite laminates.
- Because of the high degree of overlap between the data sets of drilling thrust and torque, test of hypothesis was used to evaluate the effect of workpiece temperature, speed and feed rate on the drilling thrust and torque of the Kevlar laminates

- Average value of the maximum thrust force was found to increase with the decrease in workpiece temperature under all machining conditions because of the cooling of the fiber and resin that resulted in an increase in their strength and stiffness. This can also be due to the difference in thermal expansion coefficients of the resin and the fiber which induces a compressive stress on the fiber and strengthens the bond between the fiber and resin.
- The effects of speed and feed rate on the maximum drilling thrust force have been evaluated using test of hypothesis at 95% confidence. For all levels of drilling temperature and feed rates it was observed that increasing speed from 1200 to 3000 rpm decreases the average value of maximum thrust force. This can be due to large amount of heat at high speeds that decreases the strength of the workpiece. At both levels of speeds (low and high), it was observed that increase in feed from 0.025 to 0.1 mm/rev increases the average value of maximum thrust force for all levels of drilling temperature. This can be due to the extrusion action at the chisel edge at higher feed which forms the larger fraction of the total thrust force and increases drastically with feed.
- Average value of the maximum drilling torque was found to increase with the decrease in workpiece temperature under all machining conditions because of the changed material behavior at low temperatures.
- The effects of speed and feed rate on the maximum drilling torque have been evaluated using test of hypothesis at 95% confidence. For all levels of drilling temperature and low feed rates it was observed that increasing speed from 1200 to

3000 rpm decreases the average value of maximum drilling torque. But for higher feed rates the decrease was significant up to -60^{0}C workpiece temperature, below this temperature there seem to be increase in drilling torque with the speed. At low levels of speeds, it was observed that increase in feed decreases the average value of maximum drilling torque for all levels of drilling temperature. While for high levels of speed increase in feed increases the maximum drilling torque value. This can be due to the fact that at lower workpiece temperatures the cutting force works mostly at the extreme drill radius whereas in normal situations it remains more distributed reducing the effective torque arm.

- It was found that the specific cutting energy for drilling Kevlar laminates varies inversely with the product of feed rate and drill diameter. The slopes for the laminates drilled at low temperatures were found to be significantly steeper than for dry ones showing higher machining effort. The mean slopes of curves relating the specific cutting energy with (fxd) for tested specimen ranges from -0.14 to -0.51.

Drilled holes were investigated to evaluate their quality at different machining conditions and following observations were made

- The variation of delamination factor 'F_d' with the number of holes drilled at a certain workpiece temperature was found to be represented by a normal distribution. At room temperature, the value of the 'F_d' was found to fluctuate around a higher average value compared to that of the other three workpiece

temperatures (0^0C, -60^0C, -120^0C) indicating an improvement of about 400% in the delamination damage at lower workpiece temperature.

- Average value of the 'F_d' was found to decrease with the decrease in workpiece temperature under all machining conditions because at low temperature Kevlar^{TM} laminate material has a changed behavior due to the difference of thermal expansion coefficients of the resin and matrix and also helps in changing the failure mode from bending induced rupture to shear fracture which produce a cleaner hole.
- The effects of speed and feed rate on the average value of the 'F_d' have been evaluated using test of hypothesis at 95% confidence. For all levels of drilling temperature and feed rates it was observed that increasing speed from 1200 to 3000 rpm decrease the average value of 'F_d'. But for both speeds levels, it was observed that increase in feed increases the average value of delamination factor for all levels of drilling temperature except at 0^0C.

The concepts developed in this study can be further applied to machine other composites and alloys for various operations like grinding, turning, milling etc.

REFERENCES

1. K. Uehara and S. Kumagai, “Chip Formation, Surface Roughness and Cutting Forces in Cryogenic Machining” Annals of CIRP, vol.17, no.1, pp 409-416, 1968.
2. R. Jainbajranglal and A.B. Chatopadhyay, “Role Of Cryogenics In Metal Cutting Industry” Indian Journal of Cryogenics, vol.9, no.1, pp 42-46, 1984.
3. H. Hocheng, C.K. Dharan, “Delamination during Drilling in Composite Laminates” ASME. Journal of Engineering for Industry, vol. 112, pp.236-239, 1990.
4. D. Bhattacharyya, M.N. Allen, S.J. Mander, “Cryogenic Machining of Kevlar Composites” Processing and Manufacturing of Composite Materials, vol. 27, pp 133-147, 1991.
5. S.Y. Hong, “Economical Cryogenic Machining for High Speed Cutting of Difficult to Machine Materials” Proceedings of First International Conference on Manufacturing Technology Hong Kong, pp 27-29, Dec 1991.
6. C. Evans, “Cryogenic Diamond Turning of Stainless Steel” Annals of CIRP, vol.40. no.1, pp 571-575, 1991.
7. Di Ilio A, Tagliaferri V, Veniali F, “Cutting Mechanisms in Drilling of Aramid Composites” International Journal of Machine Tools & Manufacture, Vol.31, no.2, pp 155-165, 1991.
8. Z. Zhao and S.Y. Hong, “Cooling Strategies for Cryogenic Machining from Materials View Point” Journal of Materials Engineering and Performance, vol.1, no.5, pp 669-678, 1992.
9. Z. Zhao and S.Y. Hong, “Cryogenic Properties of Some Cutting Tool Materials” Journal of Materials Engineering and Performance, vol.1, no.5, pp 705-714, 1992.

10. H. Hocheng and H.Y. Pwu, “On Drilling Characteristics of Fiber Reinforced Thermosets and Thermoplastics” International Journal of Machine Tools and Manufacture, Vol.32, No.4, pp. 583-592, 1992.
11. Bhattacharyya D., Allen M.N, S.J. Mander, “Cryogenic Machining of Kevlar Composites” Materials and Manufacturing Processes, vol. 8, no. 6, pp 631-651, 1993.
12. H. Hocheng, H.Y. Pwu, and K.C. Yao, “Machinability of Some Fiber Reinforced Thermoset and Thermoplastics in Drilling” Materials and Manufacturing Processes, vol.8, no.6, pp 653-662, 1993.
13. H.Y. Puw, and H. Hocheng, “Machinability Test of Carbon Reinforced Plastics in Milling” Materials and Manufacturing Processes, vol.8, no.6, pp 717-729, 1993.
14. N. Bhatnagar, N.K. Naik, and N. Ramakrishnan, “Experimental Investigation of Drilling on CFRP Composites” Materials and Manufacturing Processes, vol.8, no.6, pp 683-701, 1993.
15. Jain S, Yang D.C.H, “Effects of Feed Rate and Chisel Edge on Delamination in Composite Drilling” ASME, Journal of Engineering for Industry, vol.115, pp 398-405, Nov. 1994.
16. Jain S, Yang D.C.H, “Delamintion-Free Drilling of Composite Laminates” ASME Journal of Engineering for Industry, vol.116, pp 475-481, Nov. 1994.
17. Okimichi Yano and Hitoshi Yamaoka, “Cryogenic Properties of Polymers” Progress in Polymer Science, vol.20, pp 585-613, 1995.
18. Liu Fei, Kang Gewenga, Xu Zongjun “Temperature Field Control Principle and Control Models for Cryogenic Machining System” Chinese Journal of Mechanical Engineering, vol.8, No.3, pp 222-227, 1995.
19. S.Y. Hong, Y.C. Ding, “A Study of the Cutting Temperatures in Machining Processes Cooled by Liquid Nitrogen” Technical papers of NAMRI, pp 115-119, 1995.
20. S. Paul, A.B. Chattopadhyay, “Effects of Cryogenic Cooling by Liquid Nitrogen Jet on Forces, Temperature and Surface Residual Stresses in Grinding Steels” Cryogenics, vol.35, pp 515-523, 1995.

21. Caprino G, Tagliaferri V, “Damage Development in Drilling Glass Fibre Reinforced Plastics” International Journal of Machine Tools & Manufacture, vol.35, no.6, pp 817-829, 1995.
22. Chandrasekharan V, Kapoor S.G, DeVor R.E, “A Mechanistic Approach for Predicting the Cutting Forces in Drilling with Application to Fiber-Reinforced Composite Materials” Journal of Engineering For Industry, Vol.117, pp 559-570, Nov. 1995.
23. Bhatnagar N., Ramakrishnan N., Naik N.K. and Komanduri R., “On the Machining of Fiber Reinforced Plastics (FRP) Composites Laminates” International Journal of Machine Tools and Manufacture, Vol.35, No.5, pp. 701-706, 1995.
24. Z.Y. Wang, K.P. Rajurkar, M. Murugappan, “Cryogenic PCBN Turning of Ceramic (Si_3N_4)” Wear, vol.195, 1996.
25. S. Paul, A.B. Chattopadhyay, “Determination and Control of Grinding Zone Temperature under Cryogenic Cooling” International Journal of Machine Tools & Manufacture, vol.36, no.4, pp 491-501, 1996.
26. S. Paul, A.B. Chattopadhyay, “The Effect of Cryogenic Cooling on Grinding Forces” International Journal of Machine Tools & Manufacture, vol. 36, no.1, pp 63-72, 1996.
27. Z.Y. Wang, K.P. Rajurkar, “Wear of CBN Tool in Turning of Silicon Nitride with Cryogenic Cooling” International Journal of Machine Tools & Manufacture, vol.37, no.3, pp 319-326, 1997.
28. Wen, Chou Chen. “Some Experimental Investigations in the Drilling of Carbon Fiber-Reinforced Plastic (CFRP) Composite Laminate” International Journal of Machine Tools and Manufacture, vol.37, No.8, pp. 1097-1108, 1997.
29. David N. Collins, “Cryogenic Treatment of Tool Steel” Advanced Materials & Processes, Metals Park, Dec. 1998.
30. D. Bhattacharaya & D.P.W Horrigan, “A Study of Hole Drilling in Kevlar Composites” Composites Science and Technology, vol.58, pp 267-283, 1998.

31. Pwu H.Y & H. Hocheng, “Chip Formation Model of Cutting Fiber-Reinforced Plastics Perpendicular to Fiber Axis” Journal of Manufacturing Science & Engineering, vol.120, pp 192-196, Feb. 1998.
32. S.Y. Hong, Y.C. Ding, R.G. Ekkens, “Improving Low Carbon Steel Chip Breakability by Cryogenic Chip Cooling” International Journal of Machine Tools & Manufacture, vol.39, 1999.
33. C.R. Friedrich, “Near Cryogenic Machining of Polymethyl Methacrylate for Micro Milling Tool Development, Materials and Manufacturing Processes, vol.15, no.5, pp 667-678, 2000.
34. Z.Y. Wang and K.P. Rajurkar, “Cryogenic Machining of Hard to Cut Materials” Wear, Vol.239, pp 168-175, 2000.
35. N.R. Dhar, S. Paul, A.B. Chattopadhyay, “Improvement in Productivity and Quality in Machining Steels by Cryogenic Cooling” Proceedings of the National Conference on Precession Engineering, pp 247-255, Jan 2000.
36. Hong S.Y, Ding Y.C, “Cooling Approaches and Cutting Temperatures in Cryogenic Machining of Ti-6Al-4V”, International Journal of Machine Tools & Manufacture, vol.41 No.10, pp 1417-1437, Aug 2001.
37. S.Y. Hong and Y. Ding, “Micro-Temperature Manipulation in Cryogenic Machining of Low Carbon Steel” Journal of Materials Processing Technology, vol.116, no. 1, pp 22-30, Sp. Iss. SI, Oct 3, 2001.
38. N.R Dhar, S. Paul A.B Chattopadhyay, “Beneficial Effects of Cryogenic Cooling Over Dry and Wet Machining on Tool Wear and Surface Finish in Turning AISI 1060 Steel” Journal of Material Processing Technology, vol. 116, 2001.
39. S.Y. Hong, Irel Markus, Woo-Cheol Jeong, “New Cooling Approach and Tool Life Improvement in Cryogenic Machining of Titanium Alloy Ti-6Al-4V” International Journal of Machine Tools & Manufacture, vol.41, 2001.
40. Shane Y. Hong, “Economical and Ecological Cryogenic Machining” Journal of Manufacturing Science & Engineering, vol.123, pp 331-338, May 2001.

41. S.Y. Hong, Y.C. Ding, “Friction and Cutting Forces in Cryogenic Machining of Ti-6Al-4V” International Journal of Machine Tools & Manufacture, vol.41, no.10, pp 2271-2285, Aug 2001.
42. Ugo, Enemuoh, E., Sherif El-Gizawy, A., and Chukwujekwu Okafor, A. “An Approach for Development of Damage-Free Drilling of Carbon Fiber Reinforced Thermosets” International Journal of Machine Tools and Manufacture, 41, pp. 1795-1814, 2001.
43. A. Senthil Kumar, M. Rahman and S.L.Ng., “Effect of High-Pressure Coolant on Machining Performance” International Journal of Advance Manufacturing Technology, vol. 20, pp 83-91, 2002.
44. V. Nanda Kishore: S Paul: A B Chattopadhayay, “The Effect of Cryogenic Cooling on the Chips and Cutting Forces in Turning AISI 1040 and AISI 4320 Steels” Journal of Engineering Manufacture, vol.216, No.5, pp 713-721, 2002.
45. N.R. Dhar, S Paul, A.B. Chattopadhyay, “Role of Cryogenic Cooling on Cutting Temperature in Turning Steel” Journal Of Manufacturing Science & Engineering, vol.124, pp 146-153, Feb. 2002.
46. N.R Dhar, S. Paul, A.B Chattopadhyay, “Machining of AISI 4140 Steel Under Cryogenic Cooling-Tool Wear, Surface Roughness and Dimensional Deviation” Journal of Material Processing Technology, vol. 123, 2002.
47. S.Y. Hong, Y.C. Ding., and Jason Jeong, “Experimental Evaluation of Friction Coefficient and Liquid Nitrogen Lubrication Effect in Cryogenic Machining” Machining Science and Technology, vol.6, no.2, pp 235-250, 2002.
48. M.S. Won & C.K.H. Dharan, “Drilling of Aramid and Carbon Fiber Polymer Composites” Journal of Manufacturing Science & Engineering, vol.124, pp 778-783, Nov. 2002.
49. C.C. Tsao and H. Hocheng, “The Effects of Chisel Length and Associated Pilot Hole on Delamination when Drilling Composite Materials” International Journal of Machine Tools & Manufacture, vol. 43, pp 1087-1092, 2003.

50. G. Dini " On-Line Prediction of Delamination in Drilling of GFRP by Using a Neural Network Approach" Machining Science & Technology, vol.7, no.3, pp 295-314, 2003.
51. Shuaib et al "Drilling Forces and Specific Cutting Energy of KEVLAR 49 Composites Machined using TiN coated HSS Drills" Machining Science & Technology, vol.8, no. 2, 2004.
52. From the web site http://www.mfg.mtu.edu.
53. From the web site http://www.dmc.airliquide.com.
54. From the web site http://www.advancedcomposites.com/technology.htm
55. From the web site http://www.dupont.com/kevlar/index.html
56. Farhan Hamid thesis dissertation "Machinability Studies of Aramid Composites in Drilling" May 2000.

APPENDIX-A

FILTER DESIGN

Chebyshev Type I filter design (pass band ripple)

Description

Cheby1 designs low pass, band pass, high pass, and band stop digital and analog Chebyshev Type I filters. Chebyshev Type I filters are equi-ripple in the pass band and monotonic in the stop band. Type I filters roll off faster than type II filters, but at the expense of greater deviation from unity in the pass band.

Digital Domain

[b,a] = cheby1(n,Rp,Wn) designs an order n Chebyshev low pass digital Chebyshev filter with normalized pass band edge frequency W_n and Rp dB of peak-to-peak ripple in the pass band. It returns the filter coefficients in the length n+1 row vectors b and a, with coefficients in descending powers of z.

Normalized pass band edge frequency is the frequency at which the magnitude response of the filter is equal to -Rp dB. For cheby1, the normalized pass band edge frequency W_n is a number between 0 and 1, where 1 corresponds to the Nyquist frequency, pi radians per sample. Smaller values of pass band ripple Rp lead to wider transition widths (shallower roll off characteristics).

Analog Domain

[b,a] = cheby1(n,Rp,Wn,'s') designs an order 'n' low pass analog Chebyshev Type I filter with angular cheby1 edge frequency W_n rad/s. It returns the filter coefficients in length n+1 row vectors b and a, in descending powers of s.

Angular cheby1 edge frequency is the frequency at which the magnitude response of the filter is -Rp dB. For cheby1, the angular cheby1 edge frequency W_n must be greater than 0 rad/s.

Limitations

For high order filters, the state-space form is the most numerically accurate, followed by the zero-pole-gain form. The transfer function form is the least accurate; numerical problems can arise for filter orders as low as 15.

Algorithm

Cheby1 uses a five-step algorithm:

1. It finds the low pass analog prototype poles, zeros, and gain using the cheb1ap function.
2. It converts the poles, zeros, and gain into state-space form.
3. It transforms the low pass filter into a band pass, high pass, or band stop filter with desired cutoff frequencies, using a state-space transformation.
4. For digital filter design, cheby1 uses bilinear to convert the analog filter into a digital filter through a bilinear transformation with frequency pre-warping. Careful frequency adjustment guarantees that the analog filters and the digital filters will have the same frequency response magnitude at W_n or w_1 and w_2.

APPENDIX-B

Hypothesis Testing

Hypothesis testing is a method of inferential statistics. An experimenter starts with a hypothesis about a population parameter called the null hypothesis. Data are then collected and the viability of the null hypothesis is determined in light of the data. If the data are very different from what would be expected under the assumption that the null hypothesis is true, then the null hypothesis is rejected. If the data are not greatly at variance with what would be expected under the assumption that the null hypothesis is true, then the null hypothesis is not rejected. Failure to reject the null hypothesis is not the same thing as accepting the null hypothesis. In each problem considered, the question of interest is simplified into two competing claims / hypotheses between which we have a choice; the null hypothesis, denoted H_0, against the alternative hypothesis, denoted H_1. These two competing claims / hypotheses are not however treated on an equal basis; special consideration is given to the null hypothesis.

We have two common situations:

1. The experiment has been carried out in an attempt to disprove or reject a particular hypothesis, the null hypothesis, thus we give that one priority so it cannot be rejected unless the evidence against it is sufficiently strong.

2. If one of the two hypotheses is 'simpler' we give it priority so that a more 'complicated' theory is not adopted unless there is sufficient evidence against the simpler one.

The hypotheses are often statements about population parameters like expected value and variance. The outcome of a hypothesis test is 'reject H_0' or 'do not reject H_0'.

Null Hypothesis

The null hypothesis, H_0 represents a theory that has been put forward, either because it is believed to be true or because it is to be used as a basis for argument, but has not been proved. We give special consideration to the null hypothesis. This is due to the fact that the null hypothesis relates to the statement being tested, whereas the alternative hypothesis relates to the statement to be accepted if / when the null is rejected. The final conclusion once the test has been carried out is always given in terms of the null hypothesis. We either 'reject H_0 in favor of H_1' or 'do not reject H_0'; we never conclude 'reject H_1', or even 'accept H_1'. If we conclude 'do not reject H_0', this does not necessarily mean that the null hypothesis is true, it only suggests that there is not sufficient evidence against H_0 in favor of H_1; rejecting the null hypothesis then, suggests that the alternative hypothesis may be true.

Alternative Hypothesis

The alternative hypothesis, H_1, is a statement of what a statistical hypothesis test is set up to establish. The final conclusion once the test has been carried out is always given in terms of the null hypothesis. We either 'reject H_0 in favor of H_1' or 'do not reject H_0'; we never conclude 'reject H_1', or even 'accept H_1'. If we conclude 'do not reject H_0', this does not necessarily mean that the null hypothesis is true, it only suggests that there is not

sufficient evidence against H_0 in favor of H_1; rejecting the null hypothesis then, suggests that the alternative hypothesis may be true.

Two Sample t-test

A two sample t-test is a hypothesis test for answering questions about the mean where the data are collected from two random samples of independent observations, each from an underlying normal distribution:

$N(\mu_i, \sigma_i^2)$, where i = 1, 2

When carrying out a two sample t-test, it is usual to assume that the variances for the two populations are equal, that is: $\sigma_1^2 = \sigma_2^2 = \sigma^2$

The null hypothesis for the two sample t-test is $H_0 : \mu_1 = \mu_2$ that is, the two samples have both been drawn from the same population.

This null hypothesis is tested against one of the following alternative hypotheses, depending on the question posed.

$H_1 : \mu_1 \neq \mu_2$
$H_1 : \mu_1 > \mu_2$
$H_1 : \mu_1 < \mu_2$

Example of t-test performed on the data obtained from drilling of Kevlar laminate at dry and cryogenic environments.

We evaluate the effect of temperature by testing the null hypothesis $H_0 : \mu_1 - \mu_2 \leq 0$ that the mean of the thrust force of laminate 'S_a', denoted μ_1, is less than

that of S_c, denoted by μ_2, against the alternative hypothesis of H_1: $(\mu_1-\mu_2) > 0$. The data for the severest test condition f_2N_2 having feed of 0.1 mm/rev and speed 3000 rpm is used for this test. Table 4.7 shows that the average value of the thrust force for S_a is $\overline{x_1} = 116.86$ N, the standard deviation s_1 =15.78, and the sample size $n_1 = 60$, which are the number of holes drilled through S_a. On the other hand, S_c has an average thrust force $\overline{x_2} = 240.35$ N, standard deviation s_2 =36.72, and sample size $n_2 = 60$.

We first test the hypothesis that the thrust force data of S_a and S_c at drilling condition f_2N_2, are alike as to the variance using the null hypothesis ($H_0 : \sigma_1^2 = \sigma_2^2$), the alternate hypothesis ($H_1 : \sigma_1^2 > \sigma_2^2$), the rejection region $F_0 > F_{\frac{\alpha}{2},\upsilon_1,\upsilon_2}$, and the test statistics $F_0 = \frac{s_1^2}{s_2^2}$. The variances of the thrust force data of σ_1^2 and σ_2^2, respectively, which are assumed unknown, $F_{\frac{\alpha}{2},\upsilon_1,\upsilon_2}$ is the F-distribution value evaluated at a level of significance of $\alpha = 0.05$ and degrees of freedoms $\nu_1 = (n_1-1)$ and $\nu_2 = (n_2-1)$.

For the above thrust force data of S_a and S_c, since the test statistic $F_0 = \frac{s_1^2}{s_2^2} = 0.184$ is less than $F_{0.025,41,41} = 1.67$, it doesn't lie in the rejection region. Hence we don't reject the null hypothesis and conclude that at 95% confidence, the thrust force data of S_a and S_c may have the same variability, i.e. equal variances.

The hypothesis to be tested next is whether the mean of the thrust force data of S_a is less or equal to that of S_c using the null hypothesis $H_0 : \mu_1 - \mu_2 \leq 0$, the alternative $H_1 : \mu_1 - \mu_2 > 0$, the rejection region $t_0 > t_{\frac{\alpha}{2}, n_1+n_2-2}$, and the test statistic $t_0 = \frac{(\bar{x}_1 - \bar{x}_2)}{s_p \sqrt{(1/n_1) + (1/n_2)}}$ where the notation $t_0 > t_{\frac{\alpha}{2}, n_1+n_2-2}$ refers to the value of the t-distribution evaluated at a level of significance $\alpha = 0.05$ and degrees of freedom $(n_1 + n_2 - 2)$. the pooled estimate of the common variance is given by: $s_p{}^2 = \frac{(n_1 - 1)s_1{}^2 + (n_2 - 1)s_2{}^2}{(n_1 + n_2 - 2)}$. Using the above data we get $t_0 = -23.93$, and $t_{\frac{\alpha}{2}, n_1+n_2-2} = 1.66$. Since t_0 is less than 1.66, it does not lie in the rejection region and we thus conclude that, at 95% confidence, the drilling thrust force data of S_a, is less than that of S_c when both laminates were drilled at test condition f_2N_2, this means that the effect of decreasing the temperature the laminates without changing the processing and machining parameters leads to an increase in the drilling thrust force. The test of hypothesis procedure was also followed to ascertain that, at 95% confidence, the drilling torque of S_a at drilling condition f_2N_2, is also less than that of S_c. The preceding results indicate that under this test conditions, decrease in Kevlar composite laminates temperature from room to cryogenic (-120^0c) leads to increase in both thrust force and torque. If in case the two data sets the variability of are not equal then there is no basis for pooling $s_1{}^2$ and $s_2{}^2$. The

test statistic, then becomes $t_0 = \dfrac{(\bar{x}_1 - \bar{x}_2) - (\mu_1 - \mu_2)_0}{\sqrt{(s_1^{\,2}/n_1) + (s_2^{\,2}/n_2)}}$ and the rejection region will be

$t_0 > t_{\alpha,\upsilon}$ where $\nu = \dfrac{(\frac{s_1^{\,2}}{n_1} + \frac{s_2^{\,2}}{n_2})^2}{\left[\dfrac{(\frac{s_1^{\,2}}{n_1})^2}{n_1 - 1} + \dfrac{(\frac{s_2^{\,2}}{n_2})^2}{n_2 - 1}\right]}$

VITAE

- Ahmed Mujahed
- Born in India.
- Permanent Address:

H.No: 23-1-76 (First Floor)

Moghalpura Hyderabad 500002,

A.P., India. Ph. 0091-40-55802547

Email: mujahed718@yahoo.com

- Received Bachelor of Engineering (B.E.) degree in Mechanical Engineering from Osmania University, Hyderabad, India 2001
- Received Master of Science (M.S.) degree in Mechanical Engineering from King Fahd University of Petroleum & Minerals, Dhahran, Saudi Arabia in 2004.